

Title

The nematode worm *C. elegans* chooses between bacterial foods exactly as if maximizing economic utility

Authors

Abraham Katzen¹, Hui-Kuan Chung^{2,3*}, William T. Harbaugh^{4*}, Christina Della Iacono¹, Nicholas Jackson¹, Stephanie K. Yu⁴, Steven W. Flavell⁴, Paul W. Glimcher^{2,3}, Shawn R. Lockery¹

1. Institute of Neuroscience, University of Oregon, Eugene OR, USA

2. Center for Neural Science, New York University, New York, NY, USA

3. Neuroscience Institute, New York University School of Medicine, New York, NY, USA.

4. Department of Economics, University of Oregon, Eugene OR, USA

5. Picower Institute for Learning and Memory, Department of Brain & Cognitive Sciences, Massachusetts Institute of Technology, Cambridge, MA, USA

* Equal contribution

Abstract

In value-based decision making, options are selected according to subjective values assigned by the individual to available goods and actions. Despite the importance of this faculty of the mind, the neural mechanisms of value assignments, and how choices are directed by them, remain obscure. To investigate this problem, we used a classic measure of utility maximization, the Generalized Axiom of Revealed Preference, to quantify internal consistency of food preferences in *Caenorhabditis elegans*, a nematode worm with a nervous system of only 302 neurons. Using a novel combination of microfluidics and electrophysiology, we found that *C. elegans* food choices fulfill the necessary and sufficient conditions for utility maximization, indicating that nematodes behave exactly as if they maintain, and attempt to maximize, an underlying representation of subjective value. Food choices are well-fit by a utility function widely used to model human consumers. Moreover, as in many other animals, subjective values in *C. elegans* are learned, a process we now find requires intact dopamine signaling. Differential responses of identified chemosensory neurons to foods with distinct growth potential are amplified by prior consumption of these foods, suggesting that these neurons may be part of a value-assignment system. The demonstration of utility maximization in an organism with a nervous system of only 302 neurons sets a new lower bound on the computational requirements for its execution, and offers the prospect of an essentially complete explanation of value-based decision making at single neuron resolution.

Introduction

One of the primary functions of the human brain is to make decisions that maximize individual *welfare*. Welfare is fundamentally subjective, based on values the individual assigns idiosyncratically, and privately, to goods and outcomes. Can welfare maximization nevertheless be investigated in objective terms? One solution to this problem is revealed preference theory (Samuelson, 1938) which identifies the patterns of behavior, observable as such, that are necessary and sufficient evidence that subjects are choosing in ways consistent with welfare maximization or, in economic terminology, *utility maximization*. These patterns have been defined mathematically by the Generalized Axiom of Revealed Preference (GARP) (Houthakker, 1950; Afriat, 1967; Varian, 1982). A growing number of studies have utilized GARP to quantify utility maximization in children and adults under a variety of economic and physiological conditions (Harbaugh, Krause and Berry, 2001; Andreoni and Miller, 2002; Burghart, Glimcher and Lazzaro, 2013; Lazzaro *et al.*, 2016).

GARP is significant for the neuroscience of decision making because it provides a definitive behavioral test for utility maximization, or its absence. This test can be applied in to almost any organism that makes

57 choices between desirable goods that incur costs. The basic concept underlying this axiom is that a max-
58 imizing agent's choices must be internally consistent. If the agent is observed to prefer X over Y when both
59 are available then, other things being equal, the agent should not also prefer Y over X, a pattern that is
60 obviously inconsistent. Importantly, internal consistency must extend to preferences revealed indirectly,
61 through transitivity. For example, an individual observed to choose X over Y and Y over Z, has indirectly
62 revealed that they should choose X over Z. If instead Z is chosen over X, then their decision making cannot
63 be an instance of goal-directed maximization in any significant sense of the term.

64
65 The number and severity of GARP violations (assuming the agent is motivated to maintain or improve its
66 welfare), has been taken as a measure of cognitive function (Camille *et al.*, 2011). It can also be correlated
67 with physical variables such as neuroanatomy and neuronal activity (Chung, Tymula and Glimcher, 2017;
68 Pastor-Bernier, Stasiak and Schultz, 2019). These studies reveal the range of insights that can be gained
69 by combining revealed preference theory and neuroscience.

70
71 To our knowledge, however, tests for utility maximization using GARP have yet to be applied to organisms
72 more amenable to mechanistic studies such as mice, zebrafish, fruit flies, and nematodes. A major goal of
73 this study was to determine whether food choices of the nematode *C. elegans*, a microscopic round worm
74 with a nervous system of only 302 neurons, are consistent with GARP and thus exhibit a form of utility
75 maximization. A positive result would establish a simple experimental system in which neuronal activity
76 correlated with utility could be manipulated both physiologically and genetically to establish behavioral cau-
77 sality. Such a finding would also be interesting from a comparative perspective, extending the domain of
78 utility-based decision making far beyond the boundaries of organisms that are generally considered to have
79 cognition.

80
81 A microscopic worm might seem a surprising choice for investigating utility maximization. However, *C. ele-*
82 *gans* possesses a sophisticated behavioral repertoire that can be organized into to three broad functional
83 categories (Faumont, Lindsay and Lockery, 2012; Yapici, Zimmer and Domingos, 2014): (1) maintenance
84 behaviors, such as feeding, defecation, mating, and egg laying; (2) escape reflexes, for avoiding life threat-
85 ening conditions such as noxious heat, ultraviolet light, high oxygen or CO₂, toxins, desiccation, and pre-
86 dation by fungi, mites, and other nematodes; and (3) habitat and resource-localization behaviors, including
87 a variety of spatial orientation strategies that enable *C. elegans* to obtain goods such as hospitable living
88 conditions and resources (e.g., food and mating partners), and to avoid inhospitable conditions and the lack
89 of resources.

90
91 *C. elegans* exhibits a considerable range of decision making behaviors (Faumont, Lindsay and Lockery,
92 2012; Yapici, Zimmer and Domingos, 2014): (1) action versus inaction, such as probabilistic withdrawal
93 responses (Culotti and Russell, 1978; Chalfie *et al.*, 1985; Shinkai, Yamamoto, Fujiwara, Tabata,
94 Murayama, Hirotsu, Daisuke D. Ikeda, *et al.*, 2011); (2) approach versus avoidance, such as when an
95 initially attractive odor or taste is made aversive by pairing it with the absence of food (Colbert and
96 Bargmann, 1995; Saeki, Yamamoto and Iino, 2001; Torayama, Ishihara and Katsura, 2007); (3) appetitive
97 choice, such as when worms are presented with a choice between benign or pathogenic food (Zhang, Lu
98 and Bargmann, 2005); and (4) choice under risk, such as when worms must decide whether to risk crossing
99 a potentially lethal chemical barrier to obtain food (Shinkai, Yamamoto, Fujiwara, Tabata, Murayama,
100 Hirotsu, Daisuke D Ikeda, *et al.*, 2011). Other examples include the choice to remain in a food patch rather
101 than to leave to find a mate (Barrios, Nurrish and Emmons, 2008) or the choice to remain in a dwindling
102 patch of food rather than leave for a possibly better patch (Bendesky *et al.*, 2011; Milward *et al.*, 2011); the
103 latter has strong parallels with optimal foraging theory (Busch and Olofsson, 2012). *C. elegans* has also
104 been shown to exhibit bounded rationality (Simon, 1957), a property it shares with humans and most other
105 animals. Its pairwise preferences for attractive odors generally obey transitivity but with a considerable
106 number of exceptions (Iwanir *et al.*, 2019). Similarly, its pairwise preferences are not generally influenced
107 by introduction of a third option in the choice set, another classical mark of rationality, but again with a
108 considerable number of exceptions (Cohen *et al.*, 2019). However, none of these preference tests provide
109 necessary and sufficient evidence for utility maximization.

110
111 We selected food choice as the behavior most favorable for studies of utility maximization in a worm. *C. ele-*
112 *gans* is an omnivorous bacterivore that mainly inhabits rotting plant material such as decaying fruits and

113 fleshy stems (Frezal and Felix, 2015). Its natural habitat contains thousands of different species of bacteria
114 (Samuel *et al.*, 2016), including many beneficial and pathogenic varieties. Each beneficial species has a
115 characteristic nutritional quality defined in terms of the growth rate of individual worms cultured on that
116 species (Avery and Shtonda, 2003; Samuel *et al.*, 2016). In contrast, pathogenic species can be lethal (Tan
117 *et al.*, 1999). Thus food choice has immediate fitness consequences for the worm, and it is reasonable to
118 expect that *C. elegans* food choices maximize fitness. Fitness is basically an objective measure of welfare.
119 In simple organisms with a limited repertoire of motivations, there is ought to be few opportunities for sub-
120 jective and objective measures of welfare to diverge. This observation offers some confidence that the
121 worm should maximize utility, or nearly so (Kacelnik, 2006).

122
123 *C. elegans* larvae hatch with little or no knowledge of the nutritional quality of bacteria (Shtonda and Avery,
124 2006). Instead, worms learn which bacteria species are better to eat by sampling what is available. For
125 example, hatchlings are equally attracted to lawns of high and medium quality bacteria but after being
126 allowed to sample both for several hours, they acquire robust preference for high quality bacteria (Shtonda
127 and Avery, 2006). Additionally, adult worms will feed more readily on beneficial bacteria remembered from
128 previous encounters than on novel beneficial bacteria, a form of latent learning referred to as the familiar
129 food effect (Song *et al.*, 2013). In another example, the preference of naïve adults for pathogenic bacteria
130 is reversed after they sample and consume them (Zhang, Lu and Bargmann, 2005). Worms can also de-
131 velop preferences over beneficial bacteria having different levels of nutritional quality. The establishment
132 of preferences through sampling suggests an association is formed between the particular mixtures of odors
133 present in particular foods and relative nutritional gain, a form of classical conditioning we refer to as *explicit*
134 *food quality learning*.

135
136 In this study we utilized GARP to test for utility maximization and investigated its behavioral and neuronal
137 mechanisms. This was accomplished by means of a microfluidic device that enabled us to offer single,
138 semi-restrained worms high and medium quality bacteria at a range of different relative abundances while
139 monitoring consumption electrophysiologically. We found that *C. elegans* food choices in naïve and trained
140 animals are consistent with utility maximization. Worms behave as if they employed an underlying repre-
141 sentation of utility which they were acting to maximize. Preference data were well fit by a utility function
142 widely used to model the behavior of human consumers. At the behavioral level, utility maximization relies
143 on a chemotaxis strategy known as *klinotaxis*. In this strategy, head bends during sinusoidal during loco-
144 motion are biased by chemosensory input such that bend are deeper on this side where attractant concen-
145 tration is greater. At the neuronal level, we found that chemosensory neurons known to modulate head
146 position are able to discriminate between high and medium quality food, and that food quality training in-
147 creases this ability. These findings establish a new model system in which to investigate the neuronal and
148 genetic basis of subjective value (the neural correlate of utility), and its behavioral expression

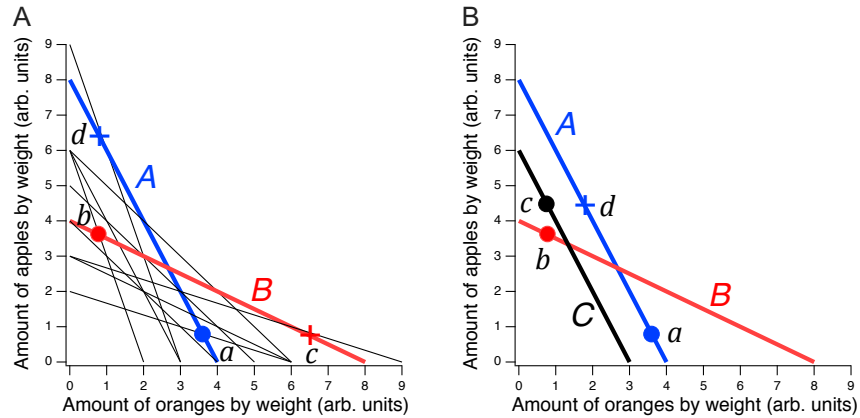
149 **Results**

150 **Results**

151 GARP for worms

152
153 In a GARP experiment for human subjects (Harbaugh, Krause and Berry, 2001), each person is given a
154 series of *choice sets*. A choice set comprises a list of options, called *bundles*, from which the person is
155 asked to pick the bundle they most prefer. Choices sets are constructed so that selections are made from
156 varying quantities of a pair of goods (e.g., apples and oranges; Fig. 1A). Each choice set is defined by a
157 unique combination of prices and budget. As each bundle consumes the entire budget (in units of money
158 or time), a bundle with more of one good has less of the other, yielding an inherent tradeoff between goods.

159
160



161

162

Figure 1. Design of a GARP experiment and tests for utility maximization

163

164

165

166

167

168

169

170

171

A. Experimental design and illustration of a direct violation of utility maximization. Diagonal lines indicate choice sets ($n = 11$). Choice sets are distinguished by having different values of the overall budget (which must be spent completely) and/or different prices for at least one of the goods. Two choice sets are highlighted by color. *A*: budget is \$8, oranges are \$2 per unit, apples are \$1 per unit; *B*: budget = \$8, oranges are \$1 per unit, apples are \$2 per unit. *Filled circles*, chosen amounts; *plus signs*, available amounts not chosen. Given the choices shown and the more is better rule, $a \succcurlyeq d > b \Rightarrow a > b$ and $b \succcurlyeq c > a \Rightarrow b > a$. The choices *a* and *b* directly violate utility maximization. **B.** Indirect violation of utility maximization. Symbols as in A. The choices *a* and *c* constitute an indirect violation of utility maximization as described in the text.

172

173 Fig. 1A shows an ensemble of such choice sets, each of which can be conceptualized as offering the two
174 goods at different prices. The lines in the figure, called *budget lines*, depict the pricing constraints and trade-
175 offs particular to each choice set. In *A*, for example, the person must forgo two units of oranges for each
176 additional unit of apples; in economic parlance, oranges in *A* are half the “price” of apples. Choosing is
177 construed as selecting the most preferred option from those available in the choice set. The constellation
178 of choices a person makes across the many different choice sets in the ensemble is analyzed for the pres-
179 ence of combinations that cannot possibly be consistent with utility maximization. We refer to these as
180 *violations* of utility maximization. The consistent absence of violations, in an ensemble containing numerous
181 choices that would violate consistency, is taken as evidence for utility maximization. Here we provide a
182 non-technical explanation of the underlying theory; technical treatments are available elsewhere (Varian,
183 1982; Harbaugh, Krause and Berry, 2001; Burghart, Glimcher and Lazzaro, 2013).

184
185 Utility violations can be direct or indirect. In the test we employ, both types of violation depend on the
186 assumption that more of a good is better than less of it (strong monotonicity of utility). The filled circles in
187 Fig. 1A are one possible pair of choices, *a* and *b*, selected to exemplify a *direct* violation. In choice set *A*, *a*
188 was selected over *d*, which was also in the choice set but was not chosen. We infer from this choice that *a*
189 is at least as good as *d*, which we write as $a \succcurlyeq d$. (We cannot conclude that *a* is better than *d* because the
190 person could have been indifferent between them, with *a* being chosen randomly.) Noting that *d* has the
191 same number of oranges but more apples than *b*, we infer by strong monotonicity that *d* is *strictly* preferred
192 to *b*, written as $d \succ b$. Combining the inferences $a \succcurlyeq d$ and $d \succ b$, we conclude that *a* should be strictly preferred
193 to *b*, that is, it should also be true that $a \succ b$. This preference is said to be revealed *directly*, because
194 when people choose *a*, they do so over another option on the same budget line, *d*, that has more of at least
195 one of the goods than *b*. Similar logic applies to choice set *B* such that *b* is directly revealed preferred to *a*,
196 that is, $b \succ a$. These two preferences constitute a violation because they are inconsistent; there is no un-
197 derlying maximization process of any kind that could allow for this combination of preferences.

198
199 A person *indirectly* reveals a preference for one bundle over another when there is a *sequence* of directly
200 revealed preferences that link the two by transitivity. Fig. 1B illustrates an indirect violation of utility maxi-
201 mization. In addition to the original choices *a* and *b*, the person picked *c* in choice set *C*. We observe that
202 *c* is directly revealed preferred to *b* because it has more of at least one good than the latter, so $c \succ b$. And,
203 as before, $b \succ a$, from which we conclude by transitivity that *c* is preferred to *a*. We write this as $c \succ^* a$,
204 where the asterisk indicates indirectness. However, at the same time the person reveals $a \succcurlyeq d$ while $d \succ c$,
205 from which we conclude $a \succ c$. These two preferences constitute a violation because they are inconsistent;
206 again, no maximization process could allow for this combination of preferences. Further, it can be shown
207 that when only two goods are available, the presence of direct violations is a necessary condition for indirect
208 violations (Rose, 1958; Heufer, 2009). This fact is the foundation for the neuronal mechanism of utility
209 maximization proposed in the Discussion.

210 211 Establishment of prerequisites for GARP experiments in *C. elegans*

212
213 The foregoing examples illustrate that a GARP experiment entails the following prerequisites: (i) goods that
214 agents would like to consume, and the more the better; (ii) observations of the agent's choices of consump-
215 tion of each good at under various budget and price constraints, and (iii) decisions on intersecting choice
216 sets. The first step in this study was to develop and validate the means to fulfill these prerequisites in
217 ecologically realistic ways for *C. elegans*.

218
219 Prerequisite (i): goods. To represent the two goods in a GARP experiment, we used bacteria species having
220 high (H) and medium (M) quality as a food source, *Comamonas* and *Bacillus simplex*, respectively (Avery
221 and Shtonda, 2003; Shtonda and Avery, 2006). We chose to work with adults worms as they are easier to
222 handle and count than the L1 larvae used in previous food-choice experiments. It was initially unknown
223 whether older worms could learn new palatable food preferences, so we began by investigating the mag-
224 nitude, neuronal dependence, and mechanisms of explicit food quality learning in the developmental period
225 spanning late L3 to young adulthood.

226
227 Synchronized, late L3 worms (N2) were transferred to a training plate which contained an equal number of
228 similar sized patches of H and M foods (Fig. 2A, Trained). Preference for H versus M food was assessed

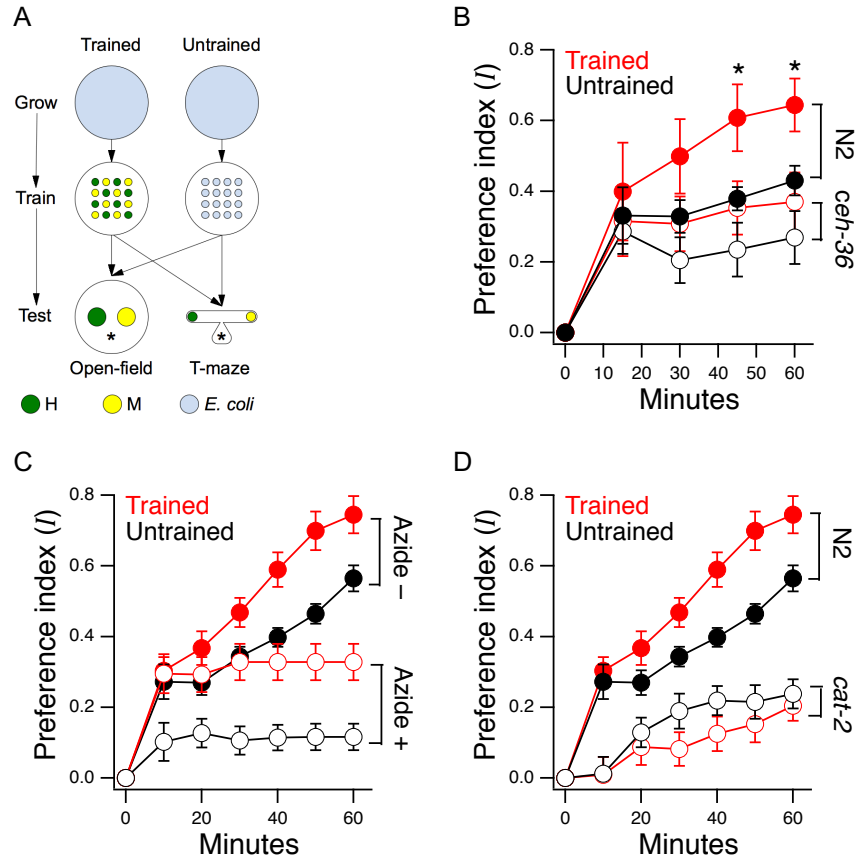
229 the following day at the young adult stage on a test plate having a single pair of H and M food patches
230 (henceforth, the “open-field accumulation assay”). Control worms were transferred to a mock training plate
231 and tested in parallel with trained worms (Fig. 2A, Untrained). Preference index I was quantified on a scale
232 such that +1 and -1 represent absolute preference for H and M food, respectively; 0 represents indifference.
233 Note that accumulation assays are not the same as the revealed preference assays used later in this study
234 to investigate utility maximization. In particular, accumulation assays do not allow worms to consume mix-
235 tures of the goods (bundles) in the same feeding bout, nor do they challenge worms with different relative
236 food densities (prices).

237
238 Trained N2 worms preferred H food to M food more strongly than untrained worms (Fig. 2B, N2, Trained
239 vs. Untrained, Supplemental Table 1¹) indicating a significant effect of food quality training. We conclude
240 that worms in the developmental period under study can learn new food preferences. However, untrained
241 N2 worms also preferred H to M food even though they were encountering these foods for the first time
242 (Fig. 2B, N2 Untrained, $I > 0$, Supplemental Table 1²). Thus, either developmental time or exposure of
243 untrained animals to *E. coli* during the growth and/or training phase of the experiment somehow induces a
244 latent preference for H over and M food at first encounter. If H food smells to the worm more like *E. coli*
245 than M food does, this preference might be explained by the so-called food familiarity effect (Song *et al.*,
246 2013), in which worms eat familiar food more readily than novel food.

247
248 *C. elegans* has 11 pairs of anterior chemosensory neurons that respond to bacteria conditioned medium
249 (Zaslaver *et al.*, 2015), acting either as on-cells (activated by onset), or off-cells (activated by offset). As a
250 first step in identifying the locus of explicit food quality learning, we measured food preferences in worms
251 with loss of function mutation in the *ceh-36* Otx homeobox gene. This gene is expressed specifically in two
252 food-sensitive chemosensory neuron pairs, AWC and ASE, where it is required for normal expression levels
253 of functionally essential genes, including chemoreceptors and ion channel subunits required for chemo-
254 transduction (Lanjuin *et al.*, 2003; Koga and Ohshima, 2004). We found that *ceh-36* worms were never-
255 theless able to distinguish H from M food, as even untrained worms exhibited a marked preference for the
256 former (Fig. 2B, *che-36*, Untrained vs. $I = 0$, Supplemental Table 1³). Moreover, this level of preference
257 was indistinguishable from that exhibited by untrained N2 worms (Fig. 2B, Trained or Untrained *ceh-36* vs.
258 N2, Untrained, Supplemental Table 1^{4,5}). However, training had no detectable effect on food preference in
259 *ceh-36* worms (Fig. 2B, *ceh-36*, Trained vs. Untrained, Supplemental Table 1⁶). Taken together, these
260 results show that undiminished *ceh-36* function is required for normal food quality learning, implicating AWC
261 and/or ASE in this process; however, full *ceh-36* function is dispensable for latent food preferences, sug-
262 gesting the other chemosensory neurons may subserve this behavior.

263
264 We next considered the mechanism of accumulation in food patches and how it may be altered by explicit
265 food quality learning. The number of worms in a food patch depends on the difference between their patch
266 entry and exit rates. In a simple experiment to study the effects of entry rate on preference index, we added
267 a fast-acting metabolic poison (sodium azide) to each food patch to prevent worms from leaving (Choi *et al.*,
268 2016). (To increase the resolution of our preference measurements, we used a T-maze baited with H
269 and M foods (Supplemental Fig. 1). The T-maze prevents worms from wandering out of range of the food
270 spots.)

271
272 Trained N2 worms tested in the absence of sodium azide preferred H food to M food more strongly than
273 untrained worms (Fig. 2C, Azide -, Trained vs. Untrained, Supplemental Table 1⁷) indicating a significant
274 effect of food quality training. In the presence of sodium azide, trained and untrained worms still accumu-
275 lated more strongly in H food than in M food (Fig. 2C: Azide+, Trained and Untrained vs. $I = 0$, Supple-
276 mental Table 1^{8,9}). This finding shows that preferences can be established on the basis of entry rate alone.
277 The decision to accumulate in a particular food can be made, at least in part, before the animal enters the
278 patch. We also observed a significant effect of training on food preference in the azide condition (Fig. 2C,
279 Azide+, Trained vs. Untrained, Supplemental Table 1¹⁰), indicating explicit food quality learning increases
280 entry rate. Finally, preference levels were substantially reduced by sodium azide (Fig. 2C, Trained, Azide+
281 vs. Azide-; Supplemental Table 1¹¹ and Untrained, Azide+ vs. Azide-; Supplemental Table 1¹²). This result
282 shows that additional mechanisms contribute to differential accumulation in H and M food, mostly likely
283 differences in exit rate, shown previously to contribute to accumulation in open-field accumulation assays
284 (Shtonda and Avery, 2006).



285
286
287
288
289
290
291
292
293
294
295
296

Figure 2. Edible bacteria act as goods over which worms form preferences through experience

A. Food quality training and preference assays. *Filled circles* represent patches of bacteria as indicated in the key. *Stars* indicate worm starting locations. **B.** Mean preference versus time for trained and untrained *ceh-36* mutants and N2 controls in open-field accumulation assays. *Stars*: significant difference between N2 Trained and Untrained (*post hoc t-test*). **C.** Mean preference vs. time for trained and untrained N2 worms in T-maze accumulation assays, with and without sodium azide in the food patches. **D.** Mean preference index vs. time for trained and untrained *cat-2(m2261)* mutants and N2 controls in T-maze accumulation assays. N2 data are from C. **A-D.** Error bars \pm SEM.

297 Explicit food quality learning in *C. elegans* is formally equivalent to a type of classical conditioning in which
298 an association is formed between the mélange of odors characteristic of particular bacteria species (Worthy,
299 Haynes, *et al.*, 2018; Worthy, Rojas, *et al.*, 2018) acting as a conditioned stimulus, and their quality as a
300 food source, acting as an unconditioned stimulus. Learning to avoid the odors of pathogenic bacteria is
301 reinforced by serotonin (Zhang, Lu and Bargmann, 2005), but less is known about how preferences for
302 palatable foods are reinforced.

303
304 We found that food quality learning is impaired in *cat-2* mutants, which have substantially reduced levels
305 of dopamine (Lints and Emmons, 1999; Sawin, Ranganathan and Horvitz, 2000; Calvo *et al.*, 2011). Pref-
306 erence for H food in untrained *cat-2* mutants was lower than in untrained N2 (Fig. 2D, Untrained, N2 vs.
307 *cat-2*, Supplemental Table 1¹³) indicating an impairment in latent learning. In addition, preference for H
308 food in trained *cat-2* mutants was lower than in trained N2 worms (Fig. 2D, Trained, N2 vs. *cat-2*, Supple-
309 mental Table 1¹⁴), indicating an impairment in explicit learning. Finally, preferences in trained and un-
310 trained *cat-2* mutants were indistinguishable (Fig. 2D *cat-2*, Trained vs. Untrained, Supplemental Table
311 1¹⁵, another indication that explicit learning was impaired.

312
313 What accounts for these impairments? Worms move more slowly when in contact with food particles, an
314 effect caused by mechanical activation of dopaminergic neurons (Sawin, Ranganathan and Horvitz, 2000;
315 Tanimoto *et al.*, 2016). Slowing is diminished in *cat-2* mutants (Sawin, Ranganathan and Horvitz, 2000;
316 Cermak *et al.*, 2020), which could cause them to exit the patch sooner than wild type worms. It is possi-
317 ble, therefore, that food quality learning in *cat-2* mutants is impaired simply because they spend less time
318 in the food, hence have less experience of it. However, we found no differences between wild type and
319 *cat-2* mutants in the proportion of time on food (Supplemental Fig. 2). This finding points to a requirement
320 for dopamine signaling in the acquisition or expression of food memory, in accordance with substantial
321 evidence showing a requirement for dopamine in other forms of associative learning in *C. elegans*
322 (Hukema, Rademakers and Jansen, 2008; Voglis and Tavernarakis, 2008; Lee, Jee and McIntire, 2009;
323 Musselman *et al.*, 2012).

324
325 GARP prerequisite (ii): quantification of consumption at particular prices. Bacteria are ingested via the
326 worm's pharynx, a rhythmically active muscular pump comprising the animal's throat. Each pharyngeal
327 contraction is called a "pump." In *C. elegans* feeding decisions, the muscular energy utilized while feeding
328 can be thought of as the functional equivalent of money or time in human budgetary experiments. Following
329 this logic, price P can be defined as the energy required to swallow the amount of bacteria ingested in a
330 single pump, $P = e/m$, where e and m are joules per pump and grams of bacterial swallowed per pump,
331 respectively. We propose m is proportional to the optical density d of the offered bacteria suspension. Ac-
332 cordingly, we modeled price of bacteria species X as

$$P_X(d_X, z_X) = e/(z_X d_X), \quad (1)$$

334
335 where z_X is a constant that converts bacteria density into grams per pump. This constant that takes into
336 account several factors: the cellular mass of the bacteria species X (grams/cell), the number of cells that
337 enter the pharynx per unit of optical density (cells/OD), and the fraction of cells entering the pharynx that
338 are passed to the gut. Equation 1 can be converted to relative price p_X by that noting energy per pump
339 should be independent of which bacteria species is being consumed, so we can set $e = 1$. Furthermore, as
340 H and M bacteria do not vary greatly in size (Avery and Shtonda, 2003), we made the simplifying assump-
341 tion that $z_H = z_M = 1$, yielding relative price

$$p_X(d_X) = 1/d_X. \quad (2)$$

342
343
344 We modeled the quantity Q of bacteria species X consumed in a feeding bout as

$$Q_X(n_X, z_X, d_X) = n_X z_X d_X, \quad (3)$$

345
346
347 where n_X is the number of pumps in food X . With $z_X = 1$ as above, relative consumption is
348

$$q_X(n_X, d_X) = n_X d_X. \quad (4)$$

For application of GARP, we computed the fractional consumption of each food, q'_X , based on the fraction of pumps spent on food X and its density in each choice set,

$$q'_X(f_X, d_X) = f_X d_X, \quad (5)$$

where $f_X = n_X / (n_H + n_M)$ and n_H and n_M are, respectively, the number of pumps in H and M food.

To measure the relationship between price and consumption, we developed a system for presenting single worms with a pair of bacteria suspensions while recording the number of pumps the worm “spends” on each (Fig. 3). The system is based on a microfluidic chip (called the “Y-chip” because of its shape) originally created to investigate the neural mechanism of klinotaxis (McCormick *et al.*, 2011), a common form of chemotaxis. *C. elegans* klinotaxis takes the form of accentuating or attenuating, respectively, locomotory head bends toward or away from attractive tastes and odors, including food (Iino and Yoshida, 2009). The Y-chip restrains the worm at the border between two liquid suspensions of bacteria (Fig. 3A,B), representing contiguous patches of food as might occur in the natural environment (Frezal and Felix, 2015). Restraint is achieved by means of a vacuum activated clamp that leaves the worm’s head, upper body, and tail free to move. The worm’s head alternates between the two streams, making sinusoidal movements that resemble crawling on a standard agarose substrate in terms of form and frequency (Supplemental Video 1).

Large movements of the worm’s head in the Y-chip made it impractical to count accurately the number of pumps in a feeding bout by optical methods (Fang-yen, Avery and Samuel, 2009; Scholz *et al.*, 2016). Instead, we counted pumps by simultaneously recording each worm’s electropharyngeogram (Raizen and Avery, 1994) via electrodes inserted into the chip (Lockery *et al.*, 2012). Despite movements of the worm’s body, normal looking EPGs were obtained, with readily identifiable excitation spikes (E) and relaxation spikes (R) (Fig. 3D). We quantified consumption of H and M food in terms of the number of pumps that occurred in each food during a 12-minute exposure to particular food offerings.

GARP prerequisite (iii): decisions from intersecting choice sets: The geometry of the Y-chip enforces the required trade-off between goods. Every swallow that occurs in H food is one that cannot occur in M food, and conversely. By systematically altering the relative concentrations of bacteria on each side of the Y-chip, we could thus alter the relative “prices” of the two kinds of bacteria (number of cells obtained per pump). This allowed us to create a series of choice sets involving different trade-off conditions, and to alter price by varying the concentrations of bacteria. In the experiments presented below we constructed choice sets that intersect, like the choice sets in Fig. 1.

Basic feeding decisions are preserved in Y-chip

A concern at the outset was the possibility that feeding in the Y-chip is not representative of feeding under standard laboratory conditions such as on agar substrates or in liquid culture. For example, the vacuum clamp likely produces mechanical stimulation, which is known to inhibit feeding (Keane and Avery, 2003). It was necessary, therefore, to assess the degree to which feeding behavior in the chip is normal. We did this by comparing the worm’s choices of what to eat and how avidly to eat it on agar plates and in the Y-chip.

Food familiarity effect. *C. elegans* pumps more rapidly in the presence of familiar bacteria than it does in the presence of unfamiliar bacteria (Song *et al.*, 2013). This effect is the result of feeding suppression triggered by the taste or smell of unfamiliar bacteria. To test for this effect in the Y-chip, we grew worms on H food or M food until young adulthood and measured pumping rates either in the same (familiar) or the converse (unfamiliar) food. We found that mean pumping rate for a given type of food was higher when that food was familiar, indicating that this aspect of feeding is intact in the Y-chip (Fig. 4A, Familiar food vs. Unfamiliar food, Supplemental Table 1¹⁶). Further, we noted that pumping rate in familiar food happened to be the same regardless of which food was familiar, allowing us to directly compare the extent to which unfamiliar food suppressed pumping rate. Interestingly, suppression was greater when the unfamiliar food

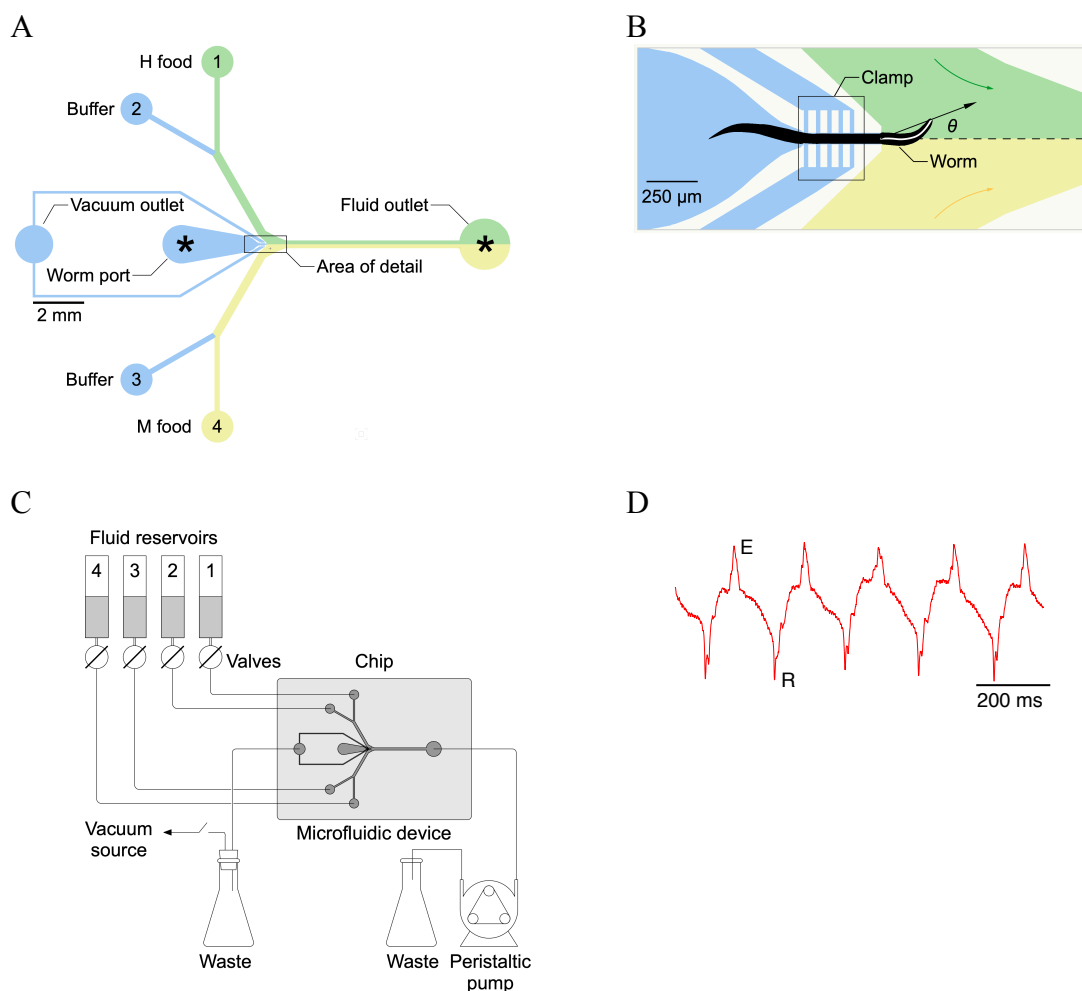
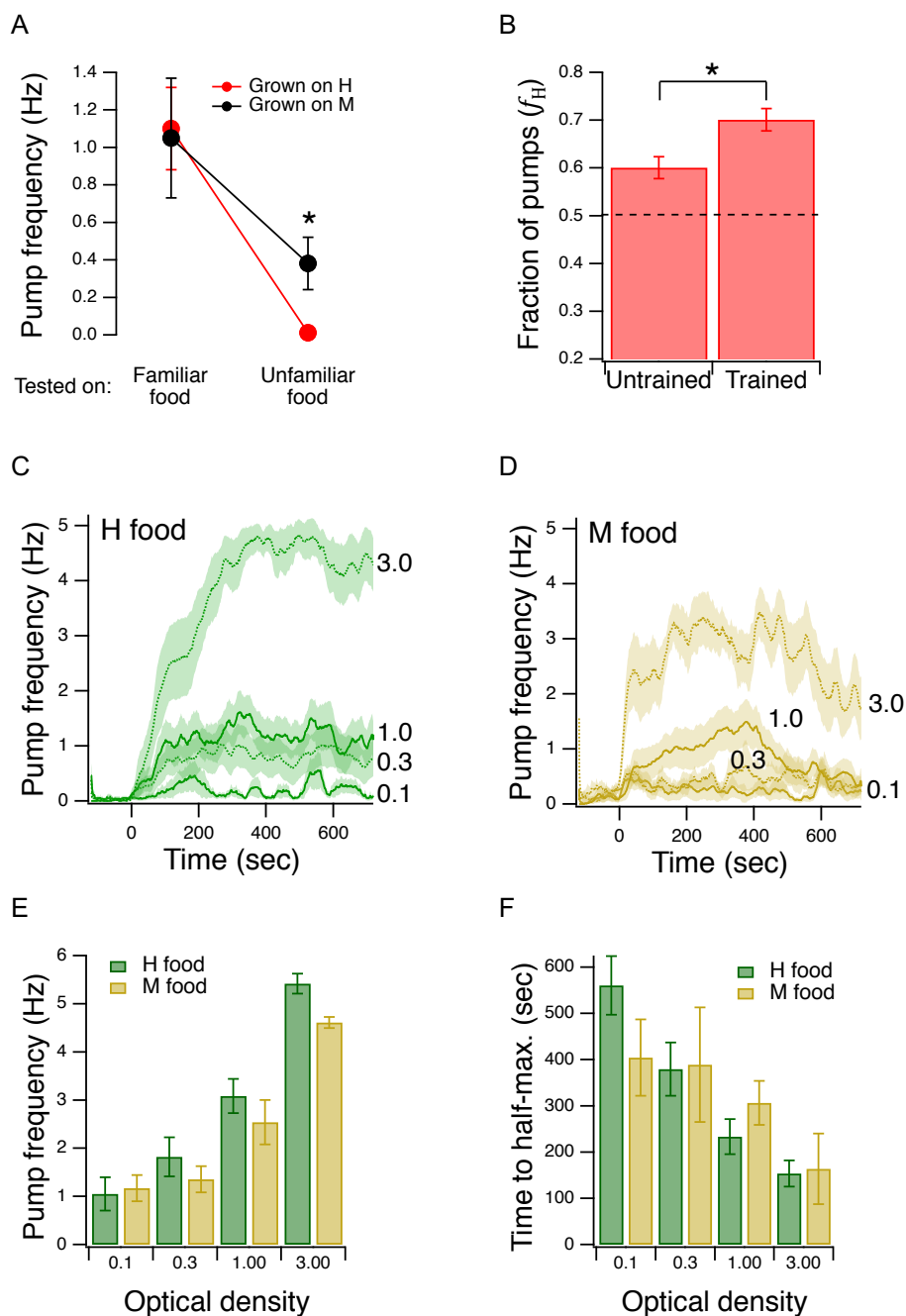


Figure 3. Single-worm food choice assays

A. Layout of the Y-chip. Asterisks indicate the position of recording electrodes. Ground electrodes (not shown) were inserted into the food and buffer ports to reduce electrical interference. The chip is shown configured for the experiments in Figs. 4B and 5B. **B.** Area of detail shown in B. The dashed line is the centerline of chip; the white line within the worm is its centerline. The black arrow connects the middle of the neck where it enters the food channel with anterior end of worm's centerline. Positive values of head angle (θ) indicate displacement toward H food. Colored arrows show direction of flow. **C.** Schematic overview of fluidic system. **D.** Typical electropharyngeogram. Each pair of excitation (E) and relaxation (R) spikes constitutes one pharyngeal pump.

402
403
404
405
406
407
408
409
410
411
412



413
414
415
416
417
418
419
420
421
422
423

Figure 4. Validation of the Y-chip for measuring food preferences

A. Familiar food effect. Mean pump frequency of worms grown on H or M food and tested on the same or the other type of food. Both foods were at OD 1. Pumping was recorded for 12 min. **B.** Food quality learning. Mean fraction of pumps in H food in trained and untrained worms. The *dashed line* indicates equal preference for H and M food. Both foods were at OD 1. **C,D.** Time course of pump frequency at four different food densities. The optical density is indicated next to each trace. **E.** Dependence of mean pump frequency on food density. **F.** Dependence of latency to half-maximal pump frequency on food density. **A-F.** Error bars and shading \pm SEM.

424
425 was lower in quality than the familiar food (Fig. 4A, Unfamiliar food, grown on H vs. grown on M, Supple-
426 mental Table 1¹⁷). This result is consistent with a model in which worms are even more reluctant to feed on
427 unfamiliar food when it is worse than what they have eaten in the recent past. A similar result has been
428 seen in the case of food-patch leaving behavior (Shtonda and Avery, 2006).

429
430 Explicit food quality learning. We tested groups of trained and untrained worms with H and M food at equal
431 concentrations (OD 1.0) in the Y-chip. Preference, as indicated by the fraction of pumps in H food (f_H , see
432 Methods), in trained and untrained worms was greater than 0.5, indicating they preferred H food in the chip,
433 just as they do in accumulation assays (Fig. 4B, Supplemental Table 1^{18,19}). Moreover, we found that this
434 preference was enhanced by training, again consistent with accumulation assays (Fig. 4B, Trained vs.
435 Untrained, Supplemental Table 1²⁰). We conclude that explicit food quality learning is intact in the Y-chip.

436
437 Effect of food density on pumping rate. Although there appear to be no systematic studies of this effect
438 when worms are feeding on bacteria lawns in petri plates, pumping rate has been shown to increase as a
439 function of food density in liquid culture (Avery and Horvitz, 1990). This effect has also been demonstrated
440 under conditions of mild restraint in microfluidic devices (Scholz *et al.*, 2016; Lee *et al.*, 2017; Weeks *et al.*,
441 2018). To test for this effect in the Y-chip, we trained worms as in Fig. 2A, except that the training plate
442 contained a single food, H or M. During testing, both channels in the Y-chip carried the food on which the
443 animals were trained (H or M) at an OD of 0.1, 0.3, 1.0, or 3.0. Pumping rate in H food was stable whereas
444 pumping rate in M appeared to decline later in the experiment (Fig. 4C,D); accordingly, we quantified pump-
445 ing in terms of its peak rate for both food types. Peak pumping rate was comparable to the rate recorded in
446 similar concentrations of *E. coli* strain OP50 under mild restraint in microfluidic devices (Scholz *et al.*, 2016;
447 Lee *et al.*, 2017; Weeks *et al.*, 2018), and exhibited the expected increase with food density (Fig. 4E; main
448 effect of OD, Supplemental Table 1²¹). We conclude that the concentration dependence of pumping rate is
449 intact in the Y-chip. This experiment also revealed previously unreported aspects of pumping kinetics. Re-
450 gardless of food type, pumping rate rose slowly, on the time scale of 100s of seconds (Fig. 4C,D). Addi-
451 tionally, we observed an inverse relationship between the latency to half-maximum pumping rate and con-
452 centration (Fig. 4F; Half-time vs. OD, Supplemental Table 1²²). Thus, worms encountering a richer food
453 source eat sooner at higher rates, a coordinated response that is presumably adaptive in natural environ-
454 ments.

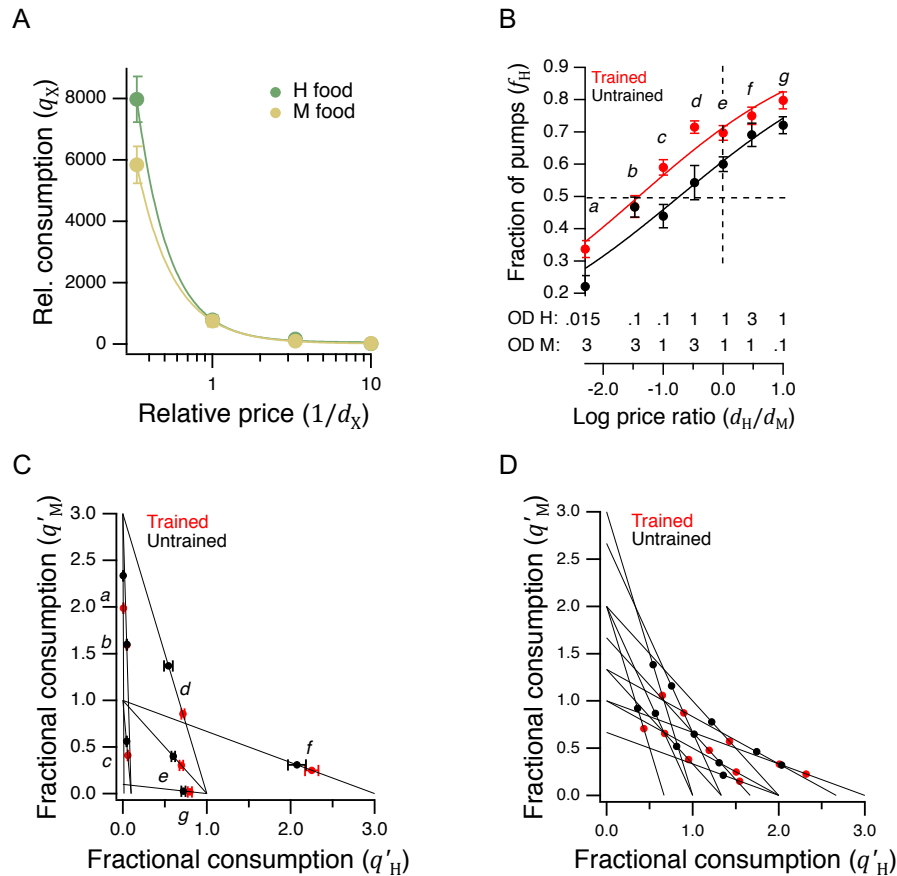
455 Demand curves

456
457 We next turned to the central question of whether *C. elegans* feeding behavior is altered by the relative
458 price of food options that vary in quality. Economists identify several different types of goods according to
459 how demand (or equivalently, consumption) is affected by changes in income or price. An *ordinary* good is
460 one for which there is an inverse relationship between price and demand. To determine whether H and M
461 food behave as ordinary goods in *C. elegans* feeding ecology, we constructed *demand curves*, in which
462 relative consumption q_x was plotted against relative price p_x for H and M food (Fig. 5A). We found an in-
463 verse relationship between mean consumption and price, indicating that H and M food do act as ordinary
464 goods, well suited to a GARP experiment.

465
466 More broadly, these results show that *C. elegans* obeys the classic law of demand, exhibiting the funda-
467 mental sensitivity of consumption to price seen in humans. The data of Fig. 5A were well fit by
468

$$469 \quad q_x(p_x) = Ap_x^\epsilon, \quad (6)$$

470
471 where A is a positive constant and $\epsilon < 0$. This is the equation for a demand curve in which the sensitivity
472 of consumption to changes in price is constant at all prices, i.e., there is constant *elasticity of demand*
473 (Varian, 1992). We found $\epsilon \cong -2$ for both food types, indicating strong elasticity, a condition that arises
474 when there many goods of nearly equivalent utility in the market. Interestingly, this may actually be the case
475 for *C. elegans*, which grows robustly on approximately 80% of the hundreds of bacteria species in its natural
476 habitat (Samuel *et al.*, 2016). Elasticity is not always the case in foraging animals. Rats exhibit inelastic
477 demand ($-1 < \epsilon < 0$) when offered only essential commodities such as food pellets and water (Kagel *et*
478 *al.*, 1975, 1981).



479 **Figure 5. Economic analysis of food choice in *C. elegans***

480
481
482
483
484
485
486
487
488
489
490
491

A. Demand curves. Mean relative consumption of familiar food versus its relative price. The data are fit by equation 6 with $\epsilon = -2.2$ for H food and $\epsilon = -1.9$ for M food. **B.** Price ratio curves. Food preference, measured as fraction of pumps in H food, versus price ratio for Trained and Untrained worms. *Horizontal dashed line*: indifference between H and M food; *vertical dashed line*: H and M food at equal price. Data at log price ratio = 0 are replotted from Fig. 4B. **C.** GARP analysis of *C. elegans* food preferences. Plotted points show mean consumption of M food versus consumption of H food in Trained and Untrained worms. Lines are choice sets as in Fig. 1. The x and y intercepts of each line indicate the amounts of H and M food that would have been consumed if the worm spent all its pumps on one or the other food type. **D.** Predicted consumption of H and M food in Trained and Untrained animals on the a widely-used ensemble containing 11 budget lines (Harbaugh, Krause and Berry, 2001). **A-C.** Error bars \pm SEM.

492

493 Integration of preference and price

494

495 In a GARP experiment, participants evaluate offerings in the choice sets by integrating their preferences
496 with constraints driven by prices. To determine if *C. elegans* performs a similar integration, we repeated the
497 experiment of Fig. 4B, now for a broad range of relative H and M prices. To avoid progressive effects of
498 feeding and satiety on food choices, each worm experienced a single choice set, and we allowed worms to
499 feed for only 12 minutes.

500

501 Data were analyzed by plotting the mean fraction of pumps spent on H food, f_H , against the log of price
502 ratio $\log(p_M/p_H)$ which, by equation 2, is equal to $\log(d_H/d_M)$. The data were fit by an exponential sigmoid
503 function of the form

504

$$f_H(r) = 1/(1 + 10^{-(r-r_0)/k}), \quad (7)$$

505

506 where r is log price ratio, r_0 is log price ratio at the point of indifference between H and M food ($f_H(r_0) =$
507 0.5), and k is the dynamic range of the function. We chose an exponential sigmoid because, like f_H , it is
508 bounded between 0 and 1. We refer to this mathematical relationship as a *price-ratio curve*. We found that
509 worms spent more pumps on H food as its relative density rose, i.e., as its relative price was reduced (Fig.
510 5B, effect of price ratio, Supplemental Table 1²³), and training shifted the price-ratio curve upward (Fig. 5B,
511 Trained vs. Untrained, Supplemental Table 1²⁴). Importantly, however, we also found that worms could be
512 induced to spend the majority of pumps on M food if the H food was made sufficiently dilute, i.e., expensive
513 (Fig. 5B, point *a*, Trained and Untrained, $f_H < 0.5$, Supplemental Table 1^{25,26}). Taken together, these data
514 show that neither food preference nor price is the sole determining factor for consumption. Instead, worms
515 appear to take both preference and price into account, as human consumers often do, and as required for
516 a GARP experiment.

517

518 Utility maximization

519

520 To apply the formal test for utility maximization to *C. elegans* food choice, we mapped the data of Fig. 5B
521 into the GARP framework by plotting mean consumption of M food against mean consumption of H food at
522 each price ratio (Fig. 5C). Under this mapping, the lines in Fig. 5C correspond to choice sets like those in
523 Fig. 1. There is one line for each price ratio. The x and y intercepts of these lines indicate the amount of
524 food (up to a scale factor) that would have been consumed had the worms spent all of their pumps on H or
525 M food, respectively. We found it impractical to standardize the number of pumps to impose a fixed energy
526 budget on each worm because of individual differences in latency to feed and mean pumping rate during
527 the recordings (Fig. 5B). We therefore plotted mean fractional consumption, q'_H and q'_M (equation 5). How-
528 ever, it is unlikely that standardization would have significantly changed experimental outcomes because
529 the relative number of pumps in each food type was stable throughout the recording period (data not
530 shown).

531

532 Following the standard method from economics, utility maximization was formally assessed according to
533 the procedure outlined by Varian (Varian, 1995). This assessment yields a single number that captures the
534 total degree of consistency of preferences. It revealed no violations in either the trained or untrained data
535 set (Fig. 5B). We provisionally concluded that worms were choosing precisely as if they were maximizing
536 utility on the seven budget lines in our study.

537

538 To assess the robustness of our finding of utility maximization, we first considered whether it could be
539 attributed to sampling error. Error bars in Fig. 5C show the standard error of the mean for consumption of
540 H food on each budget line. Given this variability, it is conceivable that one or more violations was missed
541 because of sampling error. We therefore constructed 10^8 simulated data sets by sampling from gaussian
542 distributions implied by the aforementioned standard errors. Finding no violations of utility maximization in
543 either the trained or untrained group in multiple trials, we estimate the probability of at least one violation to
544 be less than 10^{-8} . It is therefore unlikely that the absence of violations was an accident of sampling error.

545

546 However, it is conceivable that violations might have been observed if we had used a larger ensemble of
547 budget lines. To address this concern, we predicted the choices worms would make on a widely used
548 ensemble (Harbaugh, Krause and Berry, 2001; Camille *et al.*, 2011; Chung, Tymula and Glimcher, 2017),
549 which contains 11 budget lines and covers the choice space more uniformly than our 7-budget ensemble.
550 We first assessed the stringency of the 11-budget ensemble as a test for the utility maximization. This was
551 done by assuming a highly conservative null hypothesis: that worms choose completely randomly, such
552 that the fraction of pumps in H food, f_H , is drawn from a flat distribution between 0 and 1 (fraction of pumps
553 in M food was $1 - f_H$). Based on 10^6 random data sets constructed in this way, we estimate the probability
554 of a false positive finding of utility maximization (no violations) in the 11-budget ensemble to be 0.06. The
555 7-budget ensemble, by comparison, has a false positive probability of 0.87. We conclude that the 11-budget
556 ensemble is sufficiently stringent.

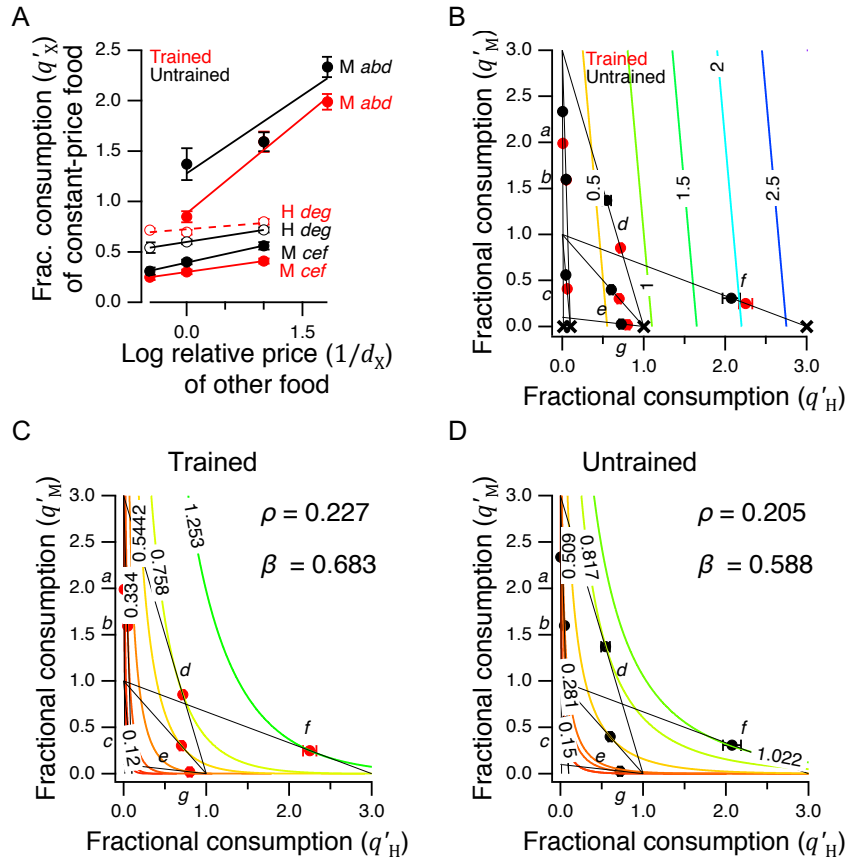
557
558 To compute how *C. elegans* would be expected to perform when choosing on the 11-budget ensemble
559 we used equation 7 to predict the expected behavior on the budget lines in Fig. 5D. Separately, we also
560 used piecewise linear representations of Fig. 5B data (not shown). In both cases we assumed that: (i) f_H ,
561 the fraction of pumps in H food is determined by relative food density, with no contribution from absolute
562 amounts of either food and (ii) that f_H is a smooth function of price ratio, to the extent implied by either
563 type of fit. Partial support for assumption (i) comes from the observation that the highest preference ob-
564 served in this study (Fig. 5A, point *g*) was obtained with mid-range optical densities. To be conservative,
565 we sampled f_H at each price ratio according the maximum standard error of the mean in the correspond-
566 ing data set in Fig. 5B (Trained or Untrained). The probability that worms would exhibit utility maximization
567 in the 11-budget ensemble was ≥ 0.98 , regardless of training state or type of fit (equation 7 or piecewise
568 linear). We conclude that the worm's price-ratio curve likely constitutes a robust utility maximization strat-
569 egy.

570
571 *Higher order features of utility maximization.* Evidence that *C. elegans* is a utility maximizer (Fig. 5C, D),
572 allowed us to investigate higher order features of utility maximization considered to be properties of human
573 decisions. Ultimately, we succeeded in establishing a utility model describing what may be the underlying
574 valuation process guiding the worm's choices.

575
576 Economic theory distinguishes between two main classes of goods – *substitutes* versus *complements* –
577 according to how changes in the price or quantity of one good that a consumer possesses affects con-
578 sumption of a second good. In the case of substitutes, which are defined as being more or less interchange-
579 able from the consumer's perspective, an increase in the price of one good causes a decrease in the con-
580 sumption of that good and a compensatory increase in consumption of the other good. This occurs as
581 consumers trade some of the good whose price increased for more of the alternative good. Pairs of goods
582 that are traded-off at a constant exchange rate, regardless of the amounts of goods on offer, are called
583 *perfect substitutes*; black and blue pens are an example of perfect substitutes (if color is not a deciding
584 factor). In the case of complements, which are defined as goods that are more desirable when consumed
585 together rather than separately, an increase in the price of one good causes a decrease in consumption of
586 both goods. Left and right shoes of the same style and size are an example of perfect complements. Wear-
587 ing only one shoe has essentially zero utility, so increases in the price of left shoes leads to decreased shoe
588 consumption overall. Although *C. elegans* consistently ate some of both foods in our experiments, we pre-
589 dicted that H and M food should act, to some degree, as substitutes for each other, as each provides
590 nutrition.

591
592 To test this prediction, we took advantage of the design of the experiment in Fig. 5B. The seven choice sets
593 can be arranged in three groups in which the price of one food was held constant while the other food was
594 offered at three different prices. In particular, there were two groups in which the price of M food was con-
595 stant while the price H food changed (points *a, b, d*, and points *c, e, f*), and there was one group in which
596 the price of H food as constant while the price of M food changed (points *d, e, g*). We analyzed these
597 instances by plotting consumption of the food whose price was constant against the price of the other food
598 (Fig. 6A). In five out of six cases, consumption of the constant-price food increased in response to increases
599 in the price of the other food (Fig. 6A, non-zero positive slope, Supplemental Table 1²⁷⁻³²). We conclude
600 that H and M food are substitutes for *C. elegans* as predicted.

601



602

603

604

605

606

607

608

609

610

611

612

613

614

615

616

617

Figure 6. Higher-order features of utility maximization

A. H and M food act as substitutes. Consumption is plotted against price for triplets of cost ratios in which the concentration of one food was constant and the concentration of the other food was variable. *Lower case italic letters*: data points in Fig. 5B. *Capital letters*: the food whose density was constant, the consumption of which is plotted on the y-axis. *Solid lines*: regression slope different from zero ($p \leq 0.01$); *dashed lines*: slope not different from zero. **B.** H and M food are not perfect substitutes. Colored contour lines are indifference curves in a perfect substitute model (equation 8) with $\beta = 10/11$. Data points from Fig. 5C are replotted for comparison, with associated budget lines, according to the conventions of that figure. 'X' symbols indicate the point of highest utility on each budget line. **C-D.** Best fitting parameterizations of the CES function (equation 9) for Trained and Untrained animals. Each panel shows the seven the iso-utility lines that are tangent to the budget lines. Goodness of fit can be assessed by observing that the iso-utility lines are tangent to the budget lines at, or near, the data points which indicate mean consumption of H and M food, replotted from Fig. 5C. **A-D.** Error bars \pm SEM.

618 Further, we can be reasonably certain that the H and M foods used in our experiments are not *perfect*
619 *substitutes*. In the case of perfect substitutes, utility is the weighted sum of the consumed amount of each
620 good. This relationship can be described with the equation

$$621 \quad U(x, y) = \beta x + (1 - \beta)y, \quad (8)$$

622 where x and y are the amounts of each good, and β is a weighting factor between 0 and 1 (inclusive). In
623 that case, the exchange rate between the two goods, i.e., the amount of y required to compensate for giving
624 up one unit of x , is a constant, $\beta/(1 - \beta)$. For example, goods that can be substituted on a one-for-one
625 basis have an exchange rate of unity ($\beta = 0.5$). Equation 8 defines a planar utility surface that lies above
626 the positive x, y plane and passes through the origin. This plane is indicated by the colored contour lines in
627 Fig. 6B, which also contains the data of Fig. 5C for comparison. The contour lines represent iso-utility lines
628 within the plane. In economics, such lines are called *indifference curves*, because a chooser would be
629 indifferent between bundles located on the same curve, as these bundles would have the same utility. In
630 the example shown, $\beta = 10/11 > 0.5$, meaning that the slope of the plane is steeper in the direction parallel
631 to the axis indicating consumption of good x , i.e, H food in the figure. A utility maximizer will therefore
632 choose the points labeled “X” as these have the highest utility available on the associated budget line. Such
633 points are called *corner solutions*, which are situations when the chooser devotes the entire budget to a
634 one of the two options. Here, the corner solutions are arrayed along the x axis (and a hypothetical worm
635 showing this pattern of perfect substitution would spend all of its pumps eating only the H food); for $\beta < 0.5$
636 the corner solutions would be arrayed along the y -axis. The complete absence of corner solutions in our
637 data is evidence that *C. elegans* does not perceive H and M food as perfect substitutes under our condi-
638 tions, but rather as *imperfect substitutes*.

639
640
641 *A model of valuation in the worm.* In widely used models of choices made by human consumers when
642 offered imperfect substitutes, the exchange rate is not constant, but varies as a function of the amount of
643 each good offered in a particular bundle. In economics this case is often modeled by the Constant Elasticity
644 of Substitution (CES) function. In the present case the CES function takes the form

$$645 \quad U(q_H, q_M) = (\beta q_H^\rho + (1 - \beta)q_M^\rho)^{1/\rho}. \quad (9)$$

646
647 The exponent $\rho (\neq 0)$ represents the sensitivity of choosers to the fact that the more of a good they already
648 possess, the less valuable each additional unit of the good becomes; in economics, this is called *diminishing*
649 *marginal utility*. This sensitivity is inversely related to ρ . Here, as in equation 8, β captures the tradeoff
650 between the goods, now after transformation by ρ . The CES utility function is quite flexible in that it can
651 generate utility surfaces (and hence indifference curves) for perfect substitutes (when $\rho = 1$), imperfect
652 substitutes (when $-0.5 < \rho < 1$), and perfect complements ($\rho \ll -0.5$).

653
654 The best fitting parameterizations of the CES function for our data (β, ρ) are shown for trained and untrained
655 worms in Fig. 6C and D, respectively. The highest contour reached by any budget line is the one that is
656 tangent to it, and this contour constitutes the CES function’s prediction of the worm’s mean preference in
657 that choice set. The close match between model and behavior for trained and untrained worms indicates
658 that *C. elegans* food choice conforms to a widely used model of choice behavior in humans. The fact that
659 β increased shows that after training the relative value of H food was higher than before. The fact that ρ
660 increased (became more positive) indicates that worms became less sensitive to diminishing marginal util-
661 ity. Thus, not only did training make H food more attractive, it also made worms require more of it to be
662 satisfied.

663 Behavioral mechanisms of utility maximization

664
665 Having shown that the worm’s preferences are consistent with utility maximization and, like human prefer-
666 ences, modeled by the CES function, we next asked how utility is maximized at the behavioral level. As
667 noted in above, we defined preference as the fraction of pumps in H food, $f_H = N_H/(N_H + N_M)$, where N_H
668 and N_M are the number of pumps in H and M food, respectively. In one model, the behavioral expression
669 of preference is a higher pumping rate in the preferred option (the “pumping-rate model”). Alternatively, it

670 might be increased amount of time spent feeding on the preferred side (the “dwell-time model”). Because
671 the number of pumps in a given food type is equal to product of the time spent in that food and the mean
672 pumping frequency in that food, an equivalent expression for preference is

$$673 \quad f_H = \frac{F_H t_H}{F_H t_H + F_M t_M} \quad (10)$$

674 where F and t are, respectively, mean pumping frequency and mean total dwell time in the indicated food
675 type. Limiting cases are informative here. If preference depends entirely on pumping frequency, then $t_H =$
676 t_M , and equation 10 reduces to the pumping-rate model

$$678 \quad f_H = \frac{F_H}{F_H + F_M} \quad (11)$$

679 in which preference for H food occurs when $F_H > F_M$, whereas preference for M food occurs when $F_M > F_H$.
680 Plotting preference as defined by equation 11 for each animal against its actual preference, $f_H = N_H / (N_H +$
681 $N_M)$, revealed a modest but significant negative correlation (Fig. 7A, Supplemental Table 1³³). This result
682 indicates a paradoxical but weak tendency to pump more slowly in H food as preference for it increases.
683 Conversely, if preference depends entirely on time in each food, then $F_H = F_M$, and equation 10 reduces to
684 the dwell-time model

$$685 \quad f_H = \frac{t_H}{t_H + t_M} \quad (12)$$

686 in which preference for H food occurs when $t_H > t_M$, whereas preference M food occurs when $t_M > t_H$.
687 Consistent with the dwell time model, we found a strong positive correlation between preference as defined
688 by equation 12 and actual preference (Fig. 7B, Supplemental Table 1³⁴). Together, these findings eliminate
689 the support the dwell-time model and exclude the frequency model.

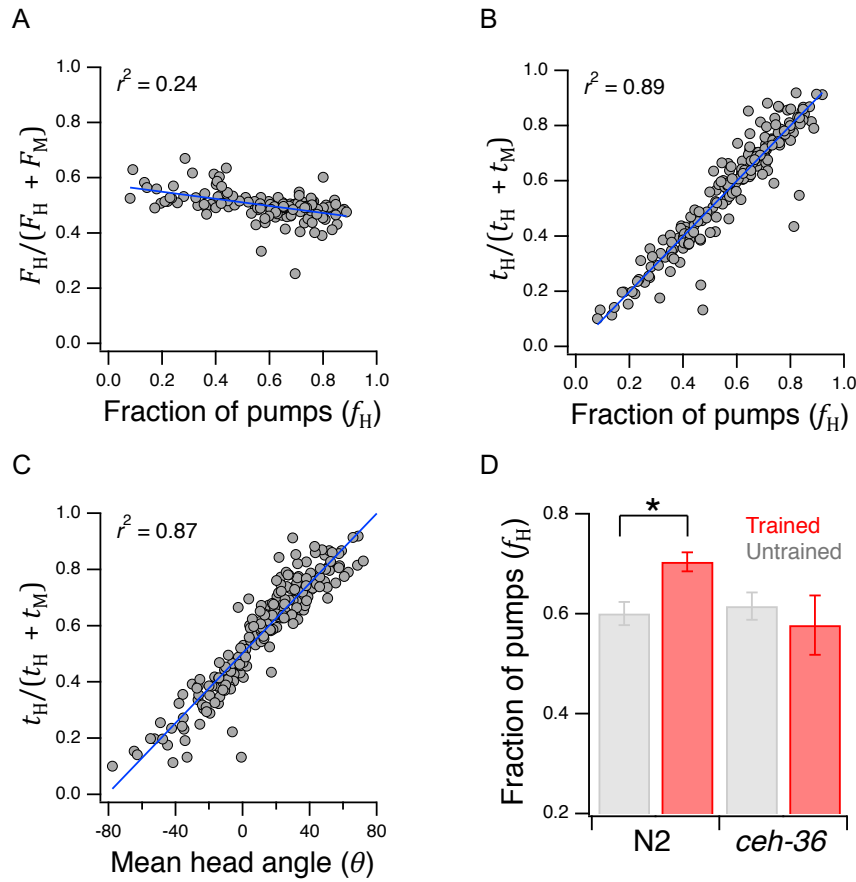
691 To determine how dwell time is biased toward the preferred food option, we measured mean head angle
692 for each animal in the data set underlying Fig. 5B. As expected, we found a strong positive correlation
693 between preference defined by equation 12 and mean head angle in the Y-chip (Fig. 7C, Supplemental
694 Table 1³⁵). Calcium imaging suggests that the angle of the worm's head with respect to the rest of the body
695 is regulated by differential activation of dorsal and ventral neck muscle motor neurons (Hendricks *et al.*,
696 2012). We propose, therefore, that the function of the neural circuit that maximizes utility is to generate
697 asymmetric activation of these motor neurons during head bends.

699 Role of chemosensory neurons in utility maximization

700 In a final series of experiments we began the search for neuronal representations of utility in *C. elegans*,
701 beginning with its chemosensory neurons.

702 *ceh-36 is required for explicit food quality learning in the Y-chip.* As shown in Fig. 4B, N2 worms preferred
703 H to M food in the Y-chip, and there was a significant effect of training. In the experiment of Fig. 7D, we
704 found that whereas untrained *ceh-36* worms also preferred H to M food (Fig. 7D, *ceh-36* Untrained, $f_H >$
705 0.5 , Supplemental Table 1³⁶), the effect of food quality training differed between N2 and *ceh-36* (Fig. 7D,
706 training \times strain, Supplemental Table 1³⁷), such that trained and untrained *ceh-36* worms were indistin-
707 guishable (Fig. 7D, *ceh-36* Trained vs. Untrained, Supplemental Table 1³⁸). These findings indicate an
708 absolute requirement for normally function in the *che-36* expressing neurons AWC and/or ASE in food
709 quality learning.

710 *Characterization of AWC's response to delivery and removal of bacteria.* We next performed a series of
711 calcium imaging experiments to characterize the worm's internal representations of H and M food. We
712 focused on AWC because it is one of the few chemosensory neuron classes known from optogenetic ma-
713 nipulation to be capable of producing precisely the type of head-angle bias that underlies the expression of
714 utility maximization in *C. elegans* (Fig. 7C)(Kocabas *et al.*, 2012). The two AWC neurons are designated



719
720
721
722
723
724
725
726
727
728

Figure 7. Behavioral mechanisms of utility maximization

A. Pumping-rate model of preference. Equation 11 is evaluated for each worm in Fig. 5B and the result is plotted against preference in terms of fraction of pumps in H food for the same animal. **B.** Dwell-time model of preference. Same as A but using equation 12. **C.** Regression of equation 12 against mean head angle as defined in Fig. 3. **A-C.** Blue lines: regressions on the data. **D.** Diminished *ceh-36* function eliminates the effect of food quality training on food preference. H and M are at OD = 1. N2 data are from Fig. 4B. Error bars \pm SEM.

729 AWC^{ON} and AWC^{OFF} according to slight differences in gene expression (Wes and Bargmann, 2001). AWC^{ON}
730 and AWC^{OFF} generate similar calcium transients to odorants that they both detect (Chalasani *et al.*, 2007);
731 for consistency, we recorded from AWC^{ON} (henceforth, "AWC"). Calcium imaging shows that AWC is inhibited
732 by bacteria conditioned medium or odorants, such as isoamyl alcohol, that are released by attractive
733 bacteria (Worthy, Haynes, *et al.*, 2018) but then responds with a robust, positive-going transient when the
734 stimulus is removed. Thus, AWC is widely considered to be food-off neuron. However, in one case, AWC
735 is known to generate an off-transient when the stimulus is switched from the odor of a preferred pathogenic
736 food, *Pseudomonas aeruginosa*, to the odor of a less preferred nonpathogenic food, *E. coli* (Ha *et al.*, 2010).
737 This finding is the first hint that AWC may be an off-neuron with more sophisticated sensitivities; here we
738 provide further evidence of this.

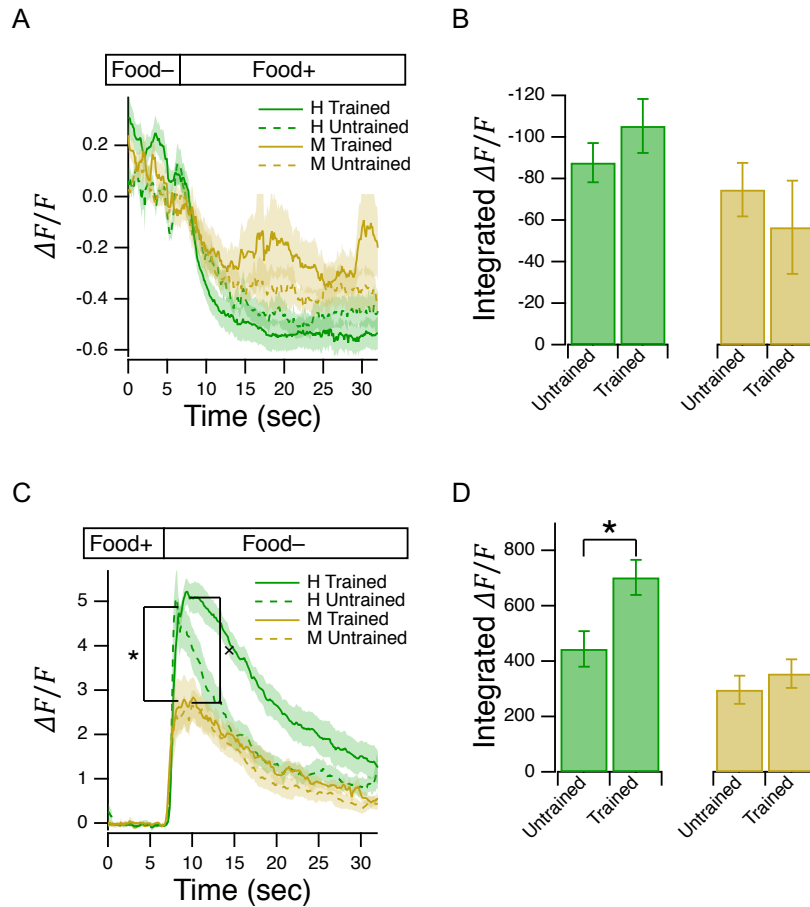
739
740 For consistency with conditions of our behavioral experiments (Fig. 2,4,5), we stimulated AWC with sus-
741 pensions of H and M bacteria. As most previous assessments of AWC's responsivity utilized either bacteria
742 conditioned medium or odorants, we first characterized AWC's responses to the delivery and removal of
743 bacteria. Such events mimic the experience of an AWC neuron when the worm moves in or out of a food
744 patch, respectively, as in our accumulation assays (e.g., Fig. 2B-D). We found, as expected from odorant
745 experiments, that AWC is inhibited by food onset (Fig. 8A) and excited by food offset (Fig. 8C) regardless
746 of food type.

747
748 Do AWC responses reflect the worm's overall preference for H? With respect to food onset, the apparently
749 stronger inhibition in response to H than M food, measured as integrated calcium response, did not reach
750 significance (Fig. 8B, effect of food type, Supplemental Table 1³⁹). However, with respect to food offset,
751 AWC was more strongly excited by H than M food (Fig. 8D, effect of food type, Supplemental Table 1⁴⁰).
752 At the more fine-grained level of peak responses within training groups, peak H food responses were sig-
753 nificantly stronger than peak M food responses (Fig. 8C, Untrained, effect of food type, asterisk, Supple-
754 mental Table 1⁴¹; Fig. 8C, Trained, effect of food type, cross, Supplemental Table 1⁴²). Overall, we conclude
755 AWC responds more strongly to removal of H food than M food. As AWC produces a bout of reverse
756 locomotion when activated (Gordus A, Pokala N, Levy S, Flavell SW, 2015), its response to food offset
757 promotes reversals, leading to increased retention patches. Our imaging data suggest that AWC-mediated
758 retention would be stronger for H than M food, promoting greater preference for H food, as seen in Fig. 2B-
759 D.

760
761 What is the effect of food-quality training on AWC responses? In the case of food onset, training appeared
762 to strengthen inhibition to H food and weaken inhibition to M food in terms of integrated responses, but this
763 trend did not reach significance (Fig. 8B, effect of training, Supplemental Table 1⁴³). In the case of food
764 offset, the results were clearer. There was a main effect of training on integrated calcium transients (Fig.
765 8D, Trained vs. Untrained, Supplemental Table 1⁴⁴), but this effect was limited to H food (Fig. 8D, H food,
766 Trained vs. Untrained, *, Supplemental Table 1^{45,46}). Overall, our imaging data suggest that AWC-mediated
767 retention in H food patches would be stronger in trained than untrained animals, promoting greater prefer-
768 ence for H food after training, as seen in Fig. 2B-D.

769
770 Imaging AWC's response to food in Y-chip assays. To mimic the experience of the worm in the Y-chip, we
771 recorded AWC responses to switching directly from one food type to the other. In the first experiment, H
772 and M food were presented at the same optical density (OD = 1). If AWC were merely a food-off neuron,
773 there should no response as food concentration did not change. On the contrary, AWC was strongly excited
774 by H→M transitions, and peak responses were amplified by food-quality training (Fig. 9A, *asterisk*, Trained
775 vs. Untrained, Supplemental Table 1⁴⁷). AWC appeared to be inhibited by M→H transitions. The extent of
776 inhibition, quantified as the integrated calcium transient, was insensitive to training (Fig. 9A, Supplemental
777 Table 1⁴⁸). Overall, we conclude that AWC is capable of reporting more than the presence or absence of
778 food, but also its identity as a preferred high-quality food source.

779
780 Taken together, the fact that normal *ceh-36* function is required for food preference in the Y-chip (Fig. 7D),
781 and that AWC is sensitive to food quality (Fig. 9A), suggest that it may provide sensory input to the worm's
782 utility maximization circuit. However, such a neuron must also be shown respond to changes in food value
783 on the time scale of individual head bends. We therefore presented worms with an alternating series of 2
784 sec step-wise presentations of H then M food. This stimulus pattern mimics the effect on AWC of head



785
786
787
788
789
790
791
792
793
794
795

Figure 8. Characterization of AWC's response to delivery and removal of food

A. Ensemble averages of relative fluorescence versus time in response to onset of the indicated food in trained and untrained animals. **B.** Summary of data in A, showing mean integrated calcium transients. **C.** Ensemble averages of relative fluorescence versus time in response to removal of the indicated food in trained and untrained animals. *Asterisk:* untrained group, mean peak response, significant difference H vs. M. *Cross:* trained group, mean peak response, significant difference H vs. M. **D.** Summary of data in C, showing mean integrated calcium transients *Asterisk:* significant difference between means. **A-D.** Shading and error bars \pm SEM.

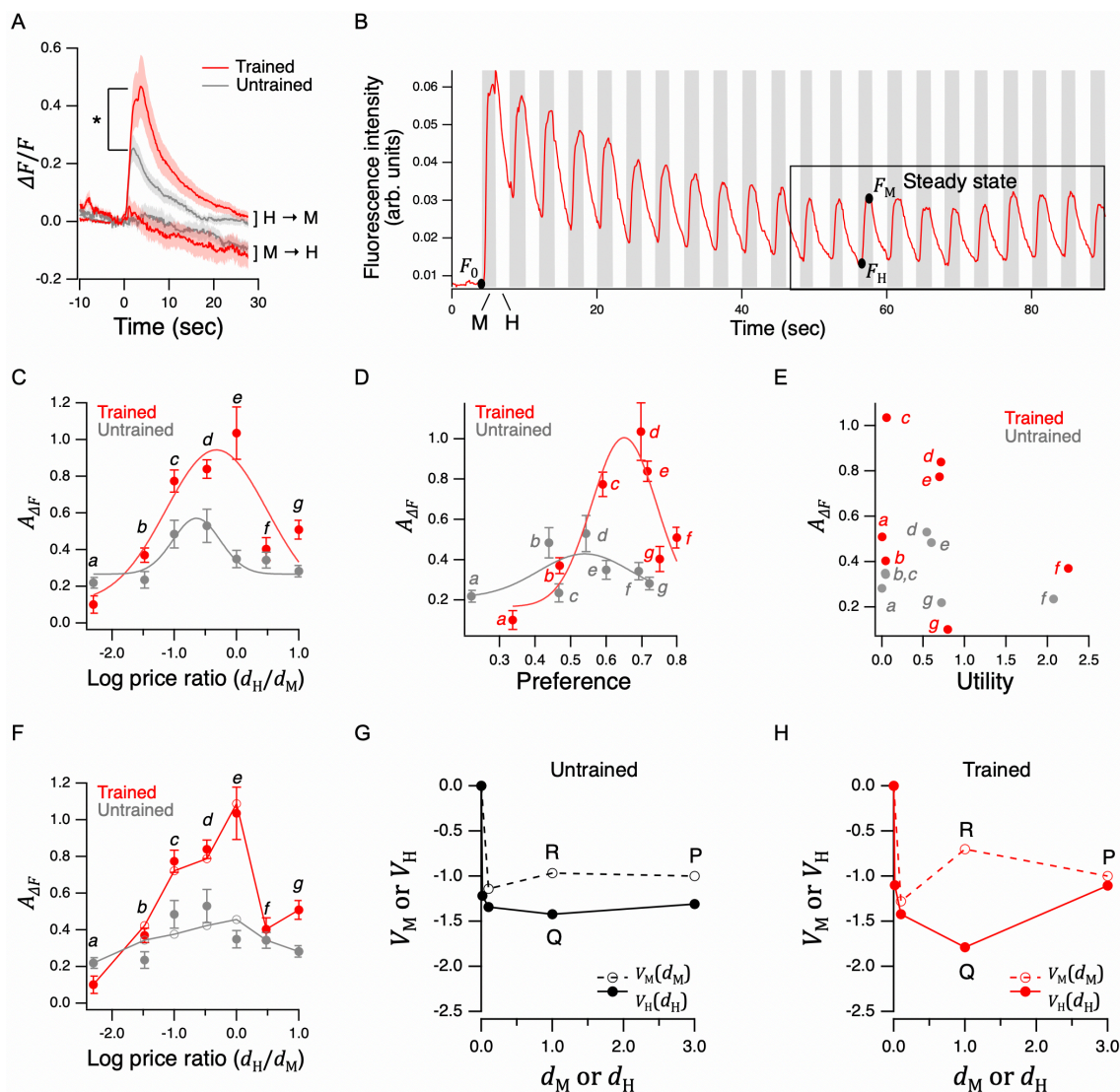


Figure 9. Characterization of AWC's response to bacteria foods in Y-chip assays.

A. Ensemble average of relative fluorescence versus time in response to transitions from H to M or M to H food. Both foods were presented at $d = 1$. Food was switched at $t = 0$. **B.** Typical fluorescence waveform in response to a series of transitions between H and M food. This stimulus approximates sensory input to the worm during a Y-chip experiment. Notation: F_0 , baseline fluorescence after sustained exposure to H food ($\cong 2$ min.); F_j , peak fluorescence following an H to M transition; F_i , trough fluorescence following an M to H transition. The box delineates the time period of presumptive steady-state behavior over which mean response amplitudes $A_{\Delta F}$ were computed for each recorded worm. **C-E.** Mean steady-state response amplitudes $A_{\Delta F}$ versus log price ratio, preference, and utility; the latter are fitted values in Fig. 6C,D. The quantity $A_{\Delta F}$ was averaged across worms within groups defined by training state (Trained vs. Untrained) and log price ratio (d_H/d_M) of presented foods. The smooth curves are gaussian fits merely to illustrate the inverted U-shaped form of the data. *Italic letters:* points in Fig. 5B. **F.** Same as C, but with lines connecting points (open circles) indicating the response amplitudes predicted by the models of AWC shown in G and H. **G-H.** Relationship between AWC membrane hyperpolarization and density of H and M food in the AWC models for trained and untrained animals. Voltage units are arbitrary. These curves underlie the predicted response amplitudes shown in F. For example, the predicted value of mean $A_{\Delta F}$ at point *d* in E is computed as the voltage at P minus the voltage at Q. Similarly, $A_{\Delta F}$ at point *e* in E is computed as the voltage at R minus the voltage at Q. **A-E.** Shading and error bars \pm SEM.

797 bends across the two food streams in the Y-chip, without the potentially confounding effects of changes in
798 dwell time at different price ratios (Fig. 7B).

799
800 The imaging trace in Fig. 9B illustrates a typical fluorescence waveform in the experiment. AWC responded
801 at two distinct time scales. On the longer time scale, it exhibited a positive transient that decayed over tens
802 of seconds, reminiscent of the time course of responses to sustained changes from H to M food (Fig. 9A).
803 On the shorter time scale, AWC responded with positive-going transients at each H→M transition, and
804 negative-going transients at each M→H transition. The fact that positive transients occurred at the H→M
805 transition, not the M→H transition, is consistent with AWC having a role in truncating head bends into the
806 non-preferred food, as a means of biasing mean head angle toward the preferred side. The waveforms we
807 obtained closely resemble the response to alternating presentations of plain buffer and buffer containing a
808 food-related odor sensed by AWC (Kato *et al.*, 2013), suggesting the AWC perceives the transition to low
809 food quality as similar to the transition to food-free medium.

810
811 *Representational content of AWC's responses.* To investigate AWC's role in utility maximization, we
812 mapped its response function across the seven price ratios used in the GARP analysis of Fig. 5B,C. We
813 assumed that the steady-state region of the imaging trace is a reasonably accurate representation of AWC
814 activity during the 12 min. behavioral recordings in the Y-chip (Fig. 5B). We defined the amplitude of the
815 calcium transients at steady-state as the mean fractional change in fluorescence between the peak at the
816 end of an M step and its preceding trough at the end of an H step ($A_{\Delta F} = \langle (F_M - F_H) / F_0 \rangle$). Reasoning that
817 larger values of $A_{\Delta F}$ should correspond to stronger head-bend truncations, and thus greater head-position
818 bias, we expected a monotonic, increasing relationship between $A_{\Delta F}$ and price ratio, consistent with the
819 price-ratio curves of Fig. 5B. Additionally, $A_{\Delta F}$ should be approximately zero near the indifference point
820 ($f_H = 0.5$), and it should reverse sign when M is preferred over H ($f_H < 0.5$). Contrary to expectations,
821 AWC's response was an inverted U-shaped function for trained and untrained animals, non-zero near the
822 indifference point, and did not reverse sign. Training greatly increased the height of the function's peak (Fig.
823 9C, effect of training, Supplemental Table 1⁴⁹) and training appeared to cause a rightward shift in the posi-
824 tion of the peak, toward higher price ratios. Similar curves were obtained when plotting $A_{\Delta F}$ against prefer-
825 ence (Fig. 9D), whereas there was no obvious relationship between $A_{\Delta F}$ and utility, at least as inferred from
826 the fitted utility values in Fig. 6C,D (Fig. 9E).

827
828 U-shaped neuronal response functions have been observed in primate orbitofrontal cortex in plots of mean
829 firing rate against the ratio of offered amounts of two desirable juice rewards (Padoa-schioppa and Assad,
830 2006). However, regression of mean firing rate against "chosen value," i.e., the value of the particular juice
831 reward that was chosen, revealed an underlying linear relationship. For neurons having U-shaped response
832 functions, chosen value was a far better predictor of neuronal responses than all other value-related quan-
833 tities tested, including the offered value of each juice, total value of juice, difference in value between cho-
834 sen and non-chosen juices, etc. We therefore considered whether AWC's responses were linearly related
835 to chosen value or related quantities.

836
837 It is straightforward to define relative food value and related quantities in terms of the densities of H and M
838 food, together with the preference for each. For example, using the value of M food as the reference, the
839 offered values of H and M at each price ratio in Fig. 5B for worms are given by

$$840 \begin{aligned} V_M &= d_M \\ V_H &= w_T d_H \text{ or } w_U d_H, \end{aligned} \quad (13)$$

841
842 where w_T and w_U are, respectively, the ratio of food densities (d_M/d_H) at the indifference point ($f_H = 0.5$) in
843 trained and untrained animals, which can be computed by taking the inverse of r_0 in equation 7. The quan-
844 tities w_T and w_U specify the number of units of M food that are equivalent to one unit of H food (assuming
845 a linear valuation function in the vicinity of the indifference point). Alternatively, value can be equated with
846 formal utility U , as inferred from fits of the CES utility function to the data in Fig. 6C,D. The resulting defini-
847 tions of chosen value, chosen utility, and related quantities are given in Supplemental Table 2. To test
848 whether AWC represents any of these quantities, we sought linear correlations between $A_{\Delta F}$ and each
849 quantity, separately in trained and untrained animals. We found no significant correlations (Supplemental
850 Table 3), making it unlikely that AWC represents the amount, value, or utility of food options in simple form.

851
852 **Model of AWC function.** Each of the functions in Supplemental Table 2 can be viewed as a unique eco-
853 nomic model of the relationship between AWC activation ($A_{\Delta F}$) and food densities d_M and d_H . As none of
854 these models fit our imaging data, we asked whether AWC's response function could be explained by a bio-
855 physical model. We and others have noted that AWC's calcium signal falls in the presence of food (Fig.
856 8A), suggesting hyperpolarization. On the other hand, when food is removed or switched from H to M,
857 AWC's calcium signal overshoots baseline, then recovers (Fig. 9A), suggesting transient depolarization.
858 This response pattern is reminiscent of rebound excitation, a common property of a variety of neurons in
859 other organisms (Huguenard and McCormick, 2007; Roberts, Li and Soffe, 2008; Kopp-Scheinpflug,
860 Sinclair and Linden, 2018). In many cases, rebound excitation is triggered by a hyperpolarization acti-
861 vated inward current, I_h . An I_h -like current has been observed in excised patches from AWC (Nickell *et*
862 *al.*, 2002). AWC expresses a number of ion channel subunit genes that could give rise to such currents.
863 These include *chl-1* (Nehrke *et al.*, 2000), and *ocr-1*, a paralog of the TRPV homolog *osm-9* (Hoenderop
864 *et al.*, 1999; Nilius *et al.*, 2000). AWC also expresses *egl-19* and *unc-2*, which encode subunits of voltage
865 gated calcium channels. These, when triggered by rebound, could generate a calcium transient. Accord-
866 ingly, we based the model on the assumption of rebound excitation in response to H→M transitions.

867
868 The model assumes that the magnitude of rebound is proportional to the change in membrane potential
869 that occurs upon an H→M transition (reduced hyperpolarization), and that the height of the calcium transi-
870 ent is proportional to the magnitude of rebound. Formally, we modeled fluorescence changes as $A_{\Delta F} =$
871 $k \cdot [V_M(d_M) - V_H(d_H)]$, where V_H and V_M are functions relating d_H and d_M to membrane potential at the
872 end of each presentation of H and the beginning of each presentation of M in an experiment such as Fig.
873 9B. For simplicity k , which has units of $A_{\Delta F}/mV$, was set to unity and membrane potential was represented
874 in arbitrary units such that differences in V_M and V_H could be displayed directly on the $A_{\Delta F}$ axis in Fig. 9F.
875 The model was fitted by an optimization routine (Brent's method for univariate functions (Press *et al.*,
876 2007)) that sought a mapping from the three different values of d_M and the four different values of d_H in
877 Fig. 5B to a hypothetical value of membrane potential produced by these foods at each price ratio; the
878 model was fitted separately for trained and untrained animals. The only constraint on the fit was to mini-
879 mize the discrepancy between modeled and actual values of $A_{\Delta F}$ at each price ratio. We made no as-
880 sumptions as to the sign or form of the functions V_M and V_H , nor did we impose a smoothness constraint
881 on these functions. We note that this optimization problem is non-trivial, as most optical densities of H
882 and M food appear in multiple price ratios, thereby reducing the number of degrees of freedom in the
883 model. For example, $d_M = 3$ at points *a*, *b* and *d* in Fig. 5B, so V_M must be the same for each of these
884 points; similarly, $d_H = 1$ at points *d*, *e*, and *g*, so V_H must be the same at these points also.

885
886 Despite the model's simplicity, we obtained remarkably good fits to the imaging data (Fig. 9F). The model
887 explains 98.5% of the variance in trained animals. It accurately reproduces large scale trends, such as the
888 overall non-monotonicity of the relationship between $A_{\Delta F}$ and log price ratio. It also reproduces small scale
889 trends including, for example, the difference in $A_{\Delta F}$ at points *f* and *g*. In the case of untrained animals, the
890 model explains 53.6% of the variance. It reproduced the large-scale non-monotonicity in the data, but did
891 not in general recapitulate small-scale trends. This may reflect the fact that in the absence of food quality
892 training, AWC responses are somewhat weaker and more variable. A satisfying aspect of the model is that
893 V_M and V_H are biologically plausible functions of food density (Fig. 9G,H). The functions for untrained ani-
894 mals can be thought of as a hyperpolarizing response that saturates as food density increases. The func-
895 tions in trained animals can be viewed similarly, except for having exaggerated deviations from each other
896 at $d_H = d_M = 1$. These functions are testable predictions of the model.

897
898 Finally, the shapes of V_M and V_H functions suggest a novel role for AWC that is distinct from representing
899 value or utility. In untrained animals, the effect of food quality on membrane potential is modest relative to
900 the effect of the overall amount of food, suggesting that the baseline role of AWC is mainly to report food
901 quantity. In trained animals, however, the neuron becomes tuned for situations in which H and M food are
902 at similar densities ($\log(d_H/d_M) \cong 0$), where discriminating foods of different quality, now regardless of
903 price, becomes important for being able to consume more of the better option.

904
905

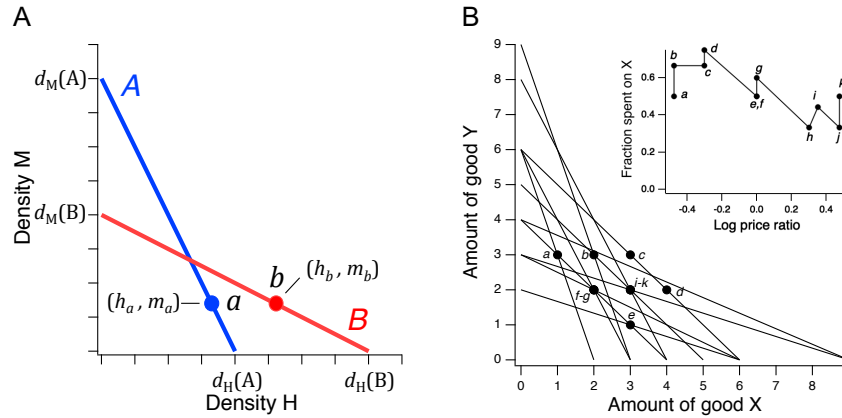
Discussion

There is growing evidence that *C. elegans* behaves as if capable of several forms of valuation including those inherent in cost-benefit decisions, transitivity of binary preferences, and independence of irrelevant alternatives (Barrios, Nurrish and Emmons, 2008; Bendesky *et al.*, 2011; Shinkai, Yamamoto, Fujiwara, Tabata, Murayama, Hirotsu, Daisuke D. Ikeda, *et al.*, 2011; Ghosh *et al.*, 2016; Cohen *et al.*, 2019; Iwanir *et al.*, 2019). The present work breaks new ground in the study of valuation in this simple organism in four key respects. (1) *C. elegans* food choices obey the classic law of supply and demand (Fig. 5A). This law has been shown to apply not just to humans but to a variety of model organisms (Kagel *et al.*, 1975; W K Bickel, L Green, 1995)(Kagel, Battalio and Green, 1995), but none as simple as *C. elegans*. (2) *C. elegans* behaves exactly as if maximizing utility (Fig. 5C). When challenged with multiple trade-offs between food quality and price, its choices satisfy the necessary and sufficient conditions for utility maximization. An organism that maximizes utility also maximizes subjective value, for it is reasonable to maximize only that which is valued. To our knowledge this is the first demonstration of value-based decision making according to GARP in an invertebrate (Fig. 5C). (3) *C. elegans* food-consumption decisions are well fit by the CES utility function (Fig. 6C,D). This function is widely used to model human consumers, but the extent to which it applies to infra-human species remains an open question (Fréchette, 2016). Here we show that the CES function accurately models consumption decisions in an organism that diverged from humans 600 million years ago (Raible and Arendt, 2004) (Fig. 6C,D), which provides new evidence of the function's universality. (4) In addition to demonstrating utility maximization in *C. elegans*, we have outlined a plausible mechanism for it. The *C. elegans* price-ratio curve is monotonic-increasing (Fig. 5B), a property that literally guarantees adherence to GARP, as discussed below (Fig. 10). Importantly, such a price-ratio curve is simple to implement at the neuronal level, requiring only that chemosensory neurons can modulate the amplitude of on-going locomotory head-bends monotonically in response to differences in food value on either side of the body.

The main limitation of the present study is high probability of a false positive finding of utility maximization in Fig. 5C. One contributing factor to this problem is the comparatively small number of budget lines in our budget ensemble, attributable to the time consuming nature of single-worm experiments with large sample sizes. Another factor is the somewhat uneven coverage of choice space, with two budget lines close to the y axis (a and b). We included these budget lines to make a stronger case for complex decision making in the worm by demonstrating preference reversals (Fig. 5B); unfortunately, this required presenting H food at very low density. We were able to address this limitation by showing that the price-ratio curve of Fig. 5B predicted the absence of transitivity violations in a larger, more stringent budget ensemble (Fig. 5D). Moreover, we show below that the absence of violations in the larger ensemble is essentially guaranteed by the monotonic form of the worm's price-ratio curve.

Distinctions between GARP and binary transitivity

Assessment of utility maximization by GARP involves demonstration of internally consistent preferences. This means non-violation of transitivity relationships inherent in directly revealed preferences, as well as those revealed indirectly through sequences of directly revealed preferences. The scientific literature on transitive choice in animals is extensive, encompassing a wide range of vertebrates: primates (Addessi *et al.*, 2008), birds (Mazur and Coe, 1987; Sumpter, Temple and Foster, 1999; Schuck-Paim and Kacelnik, 2002), and fish (Dechaume-Moncharmont *et al.*, 2013). Many invertebrates also exhibit transitivity: bees (Shafir, 1994), fruit flies (Arbuthnott *et al.*, 2017), nematodes (Cohen *et al.*, 2019; Iwanir *et al.*, 2019), and even slime molds (Latty and Beekman, 2011). However, these studies have focused almost entirely on binary transitivity, meaning either-or decisions between pairs of unitary items. Transitivity in this sense can be impressive, even in simple organisms. Choices of male fruit flies presented with pairs of genetically distinct females drawn from 10 divergent inbred strains form an inviolate transitive hierarchy of order 10 (Arbuthnott *et al.*, 2017). Striking examples notwithstanding, binary transitivity is not a sufficient condition for utility maximization. That is because in binary choices there is no notion of amount. It is therefore impossible to assess whether choices are consistent with the rule "more is better" which, as illustrated in Fig. 1A, is a necessary condition for utility maximization. Here we have demonstrated a form of transitivity in which not only the quality of goods but also their offered amount (hence price) is taken into account by the



962
963
964
965
966
967
968
969
970
971
972
973
974
975

Figure 10. Price ratio curves and utility maximization

A. A pair of intersecting budget lines wherein choices a and b are governed by price ratio curve (not shown) that is monotonic-increasing. To support a direct utility violation, a must be inside the triangle formed by B , and b must be inside the triangle formed by A . However, by monotonicity, b must lie to the right of a , for reasons described in the text. Thus, b cannot lie inside of triangle A , preventing a direct violation. **B.** Choice data from a human participant in a GARP experiment (Camille *et al.*, 2011). The data are consistent with utility maximization. *Inset*, price ratio data inferred from the experiment. Log price ratios for points a - k are calculated as $\log X_z/Y_z$, where X_z and Y_z are, respectively, the x and y intercepts of budget line z . The fraction of total budget spent on good X is computed as x_z/X_z , where x_z is the amount of good X chosen on line z .

976 organism. The full set of transitivity relationships exhibited by worms in our study is illustrated in Supple-
977 mental Fig. 3

978
979 What is being maximized?

980
981 Utility maximization raises the ineluctable question of what is being maximized. At this point, however, it is
982 easier to identify what is *not* being maximized. Three ethologically plausible maximization strategies can
983 be ruled out by simple inspection of Fig. 5C. The worm is clearly not maximizing the amount of high quality
984 food consumed, as that would have resulted in corner solutions such as those illustrated in Fig. 6B. Nor is
985 the worm maximizing the overall amount of food consumed. That would have resulted in feeding exclusively
986 in whichever of the two streams carried denser food, yielding corner solutions at the highest density on
987 each budget line (except at point e, where densities are equal and so the worm would be indifferent,
988 whereas it actually preferred H food). Finally, and perhaps surprisingly, the worm is probably not maximizing
989 its potential for rapid growth, at least in terms of a simple model in which growth rate of an individual (the
990 inverse of the number of days to grow from hatchling to day 1 adult) is proportional to the weighted sum of
991 the amounts of H and M food eaten, where the weighting factors are the observed growth rates in each
992 food type. This model fails to explain our data because growth rates in H and M food are quite similar: 0.49
993 and 0.42 days⁻¹ for H and M food, respectively (Avery and Shtonda, 2003). Such a model therefore predicts
994 an outcome similar to maximizing amount of food consumed (except at point e, where now H food would
995 be favored).

996
997 The worm's preference for non-corner solutions, called "interior solutions," is consistent with at least two
998 hypotheses concerning what *is* being maximized. Perhaps the worm is maximizing something having to do
999 with mixtures of the two foods, reminiscent of "a taste for variety" in economics (Senior, 1836; Jevons,
1000 1871). This would be an appropriate strategy if, for example, the two foods had unique essential nutrients,
1001 but we currently have no evidence for or against this. A second hypothesis is that interior solutions arise
1002 because the worm is balancing the benefit of consuming the better food option against the cost of forgoing
1003 the possibility of the sudden appearance of an even better option on the other side; this hypothesis mirrors
1004 an exploitation-exploration trade-off. Alternatively, neuro-mechanical constraints such as chemosensory
1005 transduction delays coupled with behavioral momentum (difficulty of instantaneously reversing the current
1006 head bend), could be a factor in producing interior solutions. Further work is needed to resolve this issue.

1007
1008 Establishment of subjective value assignments

1009
1010 That learning alters food preferences in *C. elegans* is well established (Ardiel and Rankin, 2010). We ex-
1011 tended these findings by showing that worms are capable of explicit food quality learning for palatable foods
1012 at least as late as larval stage L4 (Fig. 2). We also found evidence for latent acquisition of food preferences
1013 in that untrained worms encountering H and M food for the first time strongly preferred H food. The fact that
1014 this effect requires intact dopamine signaling (Fig. 2D) suggests it too may be a form of learning.

1015
1016 Explicit and latent food quality learning may be dissociable in that the former, but not the latter, exhibits a
1017 requirement for the homeobox gene *ceh-36* (Fig. 2B). In one simple model, AWC, ASE, or both neurons
1018 are loci of explicit food memories, whereas some or all of the other chemosensory neurons mediate latent
1019 learning. In partial support of this model, AWC's response to either removal of H food (Fig. 8C), or H→M
1020 transitions (Fig. 9A,C), is strongly enhanced by explicit training. It will now be important to determine
1021 whether food responses in ASE neurons are also modified by explicit training, and whether the responses
1022 of other chemosensory neurons are modified mainly by latent learning.

1023
1024 The fact that in *cat-2* mutants latent and explicit learning were reduced in trained and untrained worms (Fig.
1025 2D) implicates dopamine signaling in the acquisition or expression of food quality memories. One attractive
1026 hypothesis is that during training, dopamine neuron activity in *C. elegans* signals reward, as it does in many
1027 other organisms. In support of this model, *cat-2* is required for learned associations between salt cues and
1028 drugs of abuse that co-opt the reward systems, such as cocaine and methamphetamine (Musselman *et al.*,
1029 2012) as well acquisition of alcohol preference (Lee, Jee and McIntire, 2009). Similarly, the *C. elegans*

1030 gene *asic-1*, a member of the degenerin/epithelial sodium channel family that is mainly expressed at pre-
1031 synaptic terminals of dopaminergic neurons, is required for learned associations between tastes or odors
1032 and the presence of food (Voglis and Tavernarakis, 2008).

1033

1034 Monotonic-increasing price-ratio curves guarantee adherence to GARP

1035

1036 The price-ratio data in Fig. 5B are well fit by smooth curves that are monotonic-increasing (strictly, *non-*
1037 *decreasing*; equation 7). Here we offer a proof that a monotonic-increasing price-ratio curve precludes
1038 utility violations. In Fig. 10A, budget line *A* has the steeper slope of the two lines. Point *a* represents any
1039 location on *A* such that $b > a$ could be revealed directly (meaning *a* is between the *A-B* intersection and
1040 the *x* axis; see Fig. 1A). Point *b*, on the other hand, represents any location on *B* that is consistent with
1041 monotonicity, conditioned on the location of *a*. As the slope of *B* is shallower than the slope of *A*, and
1042 price ratio $r = d_H/d_M$, *B* has the greater price ratio. Thus $r_B > r_A$, and so by monotonicity, $f_H(r_B) > f_H(r_A)$.
1043 Furthermore, by construction $d_H(B) > d_H(A)$. Finally, by equation 5, the *x* coordinates of *a* and *b* are $h_a =$
1044 $f_H(r_A) \cdot d_H(A)$ and $h_b = f_H(r_B) \cdot d_H(B)$, respectively. Given these inequalities, $h_b > h_a$, and point *b* must
1045 always lie to the right of *a*. This means *b* will always be preferred to *a*; it can never be revealed that $a > b$.
1046 Monotonicity thereby precludes direct violations and, as direct violations are necessary for indirect viola-
1047 tions (Rose, 1958; Heufer, 2009), the latter are also precluded. Thus, monotonic price-ratio curves guar-
1048 antee adherence to GARP. This logic explains our finding that when modeling *C. elegans* food choice by
1049 the worm's price-ratio curve, the probability of finding utility maximization in the 11-budget ensemble was
1050 ≥ 0.98 (the exceptions being due to sampling noise). Although monotonic-increasing price-ratio curves
1051 guarantee utility maximization, they are not necessary for it. Fig. 10B shows data from a human subject
1052 who exhibits no utility violations, yet whose price-ratio curve is clearly non-monotonic. Thus, in relying
1053 upon monotonic price-ratio curves, the worm's choice strategy may be an adaptation for rational con-
1054 sumption behavior under the constraint of limited computational capacity.

1055

1056 A neuronal mechanism of utility maximization

1057

1058 The following simple model suggests how a monotonic price-ratio curve, and thus utility maximization, could
1059 be achieved by the *C. elegans* klinotaxis circuit. The food-sensitive chemosensory off-cells (AWC, ASER,
1060 AWB, ASH, ASK) and on-cells (ASEL, AFD, AWA, ASJ, BAG, ASI, ADF) activate, respectively, when the
1061 cell's preferred stimulus is removed or delivered (Zaslaver *et al.*, 2015). The off-cells AWC and ASER are
1062 known to truncate head bends when exogenously activated (Kocabas *et al.*, 2012). The model assumes
1063 that other off-cells do likewise, whereas on-cells extend head bends. Provided that summed activations of
1064 all off-cells and on-cells are, respectively, monotonic functions of price ratio, the amplitude of head-bend
1065 truncations and extensions will also be monotonic with respect to price ratio. Given the sinusoidal kinemat-
1066 ics of *C. elegans* locomotion, this relationship necessarily extends to relative dwell time on the side of the
1067 preferred food option, thereby increasing the fraction of pumps on that side. The non-monotonic activation
1068 function of AWC (Fig. 9) could be compensated by activations of other chemosensory neurons at price
1069 ratios greater than unity. This model can now be tested by recording and stimulating neurons in the klino-
1070 taxis circuit during choices of the type studied here.

1071

1072 Conclusion

1073

1074 All animals forage so as to obtain sufficient food at minimal cost. Omnivores like humans, *C. elegans*, and
1075 other species, face the additional challenge of reconciling trade-offs between food quality and a wide variety
1076 of costs, such as energy, time (lost opportunity), and risk. Our findings expand the scope of comparative
1077 studies already in progress in ethology, behavioral ecology, and neuroeconomics to probe the limits of
1078 classical economic theory in explaining such fundamental trade-offs (Kalenscher, Wingerden and Hayden,
1079 2011; Pearson, Watson and Platt, 2014). Is the classical theory universally applicable to animal behavior?
1080 To what extent can it be grounded in neurophysiology? The small size and unequalled annotation of the
1081 *C. elegans* nervous system (White JG, Southgate E, Thomson JN, 1986; Jarrell *et al.*, 2012; Hammarlund
1082 *et al.*, 2018; Cook *et al.*, 2019; Brittin *et al.*, 2021; Hobert, 2021), coupled with recent advances in brain
1083 wide imaging in this organism (Kato *et al.*, 2015; Nguyen *et al.*, 2016; Venkatachalam *et al.*, 2016) offer
1084 unique advantages in answering these questions.

1085

1086
1087
1088
1089
1090

MATERIALS AND METHODS

Worm strains. The following genotypes were used:

Experiment	Figure	Genotype
Wild type decision making	2, 4-9	N2
Requirement for AWC/ASE neurons	2B, 7D	<i>ceh-36(ky646)</i>
Requirement for dopamine signaling	2D	<i>cat-2(tm2261)</i>
Calcium imaging from AWC neurons	9	<i>ntl1703[<i>str-2::GCamp6s-wcherry</i>; <i>unc-122::dsred2</i>]</i>
Proportion of time on food	2 (suppl.)	<i>cat-2(n4547), cat-2(e1112)</i>

1091
1092
1093
1094
1095
1096
1097
1098
1099
1100
1101
1102
1103
1104
1105
1106
1107
1108
1109
1110
1111
1112
1113
1114
1115
1116
1117
1118
1119
1120
1121
1122
1123
1124
1125
1126
1127
1128
1129

Bacteria strains. Streptomycin resistant strains of three species were used: *E. coli* (OP50 DA 837) representing standard laboratory food, *Comamonas* sp. (DA1877) representing high quality food (H), and *Bacillus simplex* (DA1885), representing medium quality food (M). To culture bacteria, a small scraping of frozen stock was transferred to 400 mL of LB broth in a 500 mL flask to which streptomycin (50 µg/mL) added to inhibit competitive bacterial growth. Cultures were grown overnight in on a shaker (3 Hz) at 35 C. Optical density (OD) of bacteria suspensions was measured at 600 nm.

Worm cultivation and training. Worms were synchronized by isolating eggs from 10 gravid adults allowed to lay eggs for five hours. Progeny were cultivated until late larval stage L3 at 20 °C on 50 cm plates containing low-density nematode growth medium (NGM; (Brenner, 1974)) seeded with standard laboratory food (*E. coli* OP50). In experiments involving *explicit food quality training*, worms were washed three times in M9 buffer, pelleted by sedimentation, then transferred in a 2 µL aliquot (~150 worms) to a training plate (50 mm diam.) filled with bactopectone-free NGM containing 200 µg/mL streptomycin. Training plates were prepared one day in advance by spotting them with eight patches each of H and M food. Patches were formed by pipetting 10 µL aliquots of bacteria culture, suspended in LB broth at OD = 10, in a 4 × 4 grid with 10 mm between patch centers (Fig. 2A). Control plates were spotted with patches of OP50 in the same pattern. Worms resided on training plates for 18-24 hours before testing. In experiments involving the *food familiarity effect*, training plates contained 16 patches of either H or M food prepared in the same way.

Accumulation assays. In *open-field assays*, NGM test plates (50 mm diameter) were spotted with one patch each of H and M food (100 µL, OD = 10) separated by 25 mm. In *T-maze assays*, a mask formed by laser cutting 2 mm thick ethylene-vinyl acetate foam sheets (Supplemental Fig. 1; Supplemental Table 4. The mask was placed on the NGM surface and baited with the same amounts of H and M food. After training, worms were washed and transferred as above to the plate center or the starting point in the T-maze. Preference at each time point was computed as $(N_H - N_M)/(N_H + N_M)$, where N is the number of worms in contact with the food-type indicated by the subscript. Worms were counted by eye with the aid of a tally counter; the experimenter was blind to condition.

Food dwell-time assays. Dwell-time on food patches was measured as described previously (Cermak *et al.*, 2020). Assay plates were standard 10 cm diameter petri dishes filled with low-peptone (0.2 g/L) nematode growth medium, seeded with 200 mL *E. coli* OP50. Low-peptone medium ensured thin bacterial lawns for improved tracking optics. Roughly circular lawns were created with a spreader, and plates were left to dry overnight before use. For recordings, a single 72 hr old adult animal was picked to an assay plate, allowed to accommodate for 10 min, and then tracked for approximately six hours at 20 fps using the described automated tracking microscope. Prior to tracking, the lawn boundary was annotated by manually circumscribing it with the microscope. This procedure enabled post-hoc determination of when the worm was on or off the lawn.

1130 *System for recording food choice in semi-restrained worms.* The system comprised (1) a food delivery
1131 system, (2) instrumentation for electrophysiological recording, and (3) a video camera for recording behav-
1132 ior (Fig. 3).

1133
1134 (1) Food delivery system. Bacteria suspensions, and bacteria-free buffer, were held in 20 mL reservoirs
1135 (syringes with plungers removed) fitted with stopcocks. Reservoirs were suspended 50 cm above the chip
1136 and connected to it via polyethylene tubing (PE-9) fitted with 1.5 mm diameter \times 12.5 mm stainless steel
1137 nipples (17 Ga, \times 0.500", New England Small Tube, Litchfield, New Hampshire). To minimize settling of
1138 bacteria, a miniature magnetic stir bar in each reservoir was agitated periodically during experiments by
1139 moving a small hand-held magnet. The layout of the Y-chip was similar in all main respects to a previous
1140 design (McCormick *et al.*, 2011); feature height was 55 μ m. Flow rate in the chip was regulated by a peri-
1141 staltic pump (model 426-2000, Labconco, Kansas City, MO, USA) attached to chip's outlet port.

1142
1143 (2) Electrophysiology. Electropharyngeograms were recorded by means of electrodes (stainless steel nip-
1144 ples, see above) inserted into the worm port and fluid outlet. In this configuration they were used to measure
1145 the voltage differences that occur between the worm's head and tail during pharyngeal muscle action po-
1146 tentials. The vacuum clamp accentuates these voltage differences by increasing the electrical resistance
1147 between head and tail. Voltage differences between electrodes were amplified by a differential amplifier
1148 (model 1700, AM Systems, Sequim, Washington) and digitized (2 kHz) for later analysis (USB-9215A, Na-
1149 tional Instruments, Austin, Texas). Digitized recordings were bandpass filtered between 5 and 200 Hz. E
1150 and R spikes were detected offline by a manually adjusted threshold in custom data analysis software.
1151 Instantaneous pumping rate was computed using a 5 sec. sliding window average (forward looking).

1152
1153 (3) Videography. The worm was imaged using a stereomicroscope (Wild M3C, Leica, Buffalo Grove, Illinois)
1154 with a 1.5 \times objective, and a video camera (VE-CCDTX, DATG MTI, Michigan City, Illinois) with a frame rate
1155 of 30 Hz. Individual frames were analyzed by MATLAB scripts (Mathworks, Natick, MA) to extract head
1156 angle of the worm as previously described (McCormick *et al.* 2011). First, each frame was thresholded to
1157 identify the worm's head and neck region, which was then skeletonized to obtain its centerline (white line,
1158 Fig. 3B) and head angle (θ) was defined as described Fig. 3B. Values of head angle when the worm was
1159 exhibiting presumptive reversal behavior (Faumont and Lockery, 2006) were excluded manually, without
1160 knowledge of experimental condition.

1161
1162 *Single-worm food choice assays.* To minimize extraneous olfactory or gustatory cues, washed bacteria
1163 were resuspended in a minimal buffer to the desired OD; the buffer contained (in mM): 1 MgSO₄, 10 HEPES
1164 adjusted 350-360 mOsm (glycerol). We found that OD = 1 respectively corresponds to approximately 2.35
1165 \times 10⁹ and 2.00 \times 10⁹ colony forming units/mL of *Comamonas* and *Simplex*, respectively. However, OD is a
1166 better proxy for mass of bacteria in a suspended sample (Koch, 1970; Stevenson *et al.*, 2016). After training,
1167 worms were washed and transferred to foodless plates for 1-2 hours of food deprivation. At the start of the
1168 assay, the Y-chip was filled with buffer solution and a worm was inserted into the chip by liquid transfer
1169 using a syringe fitting with PE tubing and a steel nipple. During a 2 min. accommodation period, both
1170 streams carried buffer and the video and electrophysiological recordings were initiated. After accommoda-
1171 tion, both streams were switched to particular food types according to the needs of the experiment. In *food-*
1172 *familiarity* (Fig. 4A) and *food-density* experiments (Fig. 4C-D) channels 1 and 4 carried the same food (H
1173 or M). In *food quality learning* (Fig. 4B) and *integration of preference and price* (Fig. 5B), channel 1 carried
1174 H food and channel 4 carried M food at optical densities given in the legends or indicated in the figures.
1175 Feeding was recorded for 12 min. after food onset. Mean pumping frequency was computed as the number
1176 of pumps (paired E and R spikes) divided by total observation time. Preference (f_H) was defined as the
1177 fraction of pumps emitted when the tip of the worm's head, where the mouth is located, was in H food, as
1178 detected in the synchronized video recording. Specifically, $f_H = N_H / (N_H + N_M)$, where N_H and N_M are the
1179 number of pumps in H and M food, respectively; on this scale, $f_H = 0.5$ constitutes equal preference for the
1180 two foods or, in economic terms, indifference between the two options.

1181
1182 *Fitting utility functions to preference data*
1183

1184 To fit the CES function (equation 9) to the choice data in Fig. 6C,D, we estimated the parameters β and ρ
1185 using two-limit tobit maximum likelihood. Values of the error term were drawn from identical and independ-
1186 ent normal distributions (Andreoni and Miller, 2002).

1187

1188 *System for calcium imaging of neuronal activity*

1189

1190 For recording from AWC neurons, the genetically encoded calcium indicator GCaMP6s was expressed
1191 under control of the *str-2* promoter. Late L4 or early adult worms were immobilized in a newly designed
1192 microfluidic imaging chip (Supplemental Fig. 4) based on a previous device in which the worm's nose pro-
1193 trudes into a switchable stimulus stream (Chronis et al., 2007). Chip feature-height was 30 μm . The chip
1194 was adapted for rapid switching. The switching time constant in a microfluidic chip that is driven by a con-
1195 stant current source (e.g., a syringe pump) is equal to the product of the system's compliance (C) and fluidic
1196 resistance of the chip (R). To reduce compliance we used rigid inlet tubing and to reduce resistance fabri-
1197 cated wide channels.

1198

1199 To improve stimulus stability, fluid flow was driven by a syringe pump rather than gravity or pressure. Two
1200 of the four syringes in the pump were filled with H food and two with M food. Syringes were connected to
1201 the chip such that if all four channels were flowing into the chip, the cross-sectional flow at the point of
1202 confluence near the worm would be $H_2 H_1 M_1 M_2$. Stimulus presentation was automated utilizing a micro-
1203 processor to control a pair of two-way solenoid valves (LFAA1201610H, The Lee Company, Westbrook,
1204 Connecticut) in series with the syringes H_1 and M_1 ; the outer channels H_2 and M_2 flowed continuously. To
1205 present H food, the stimulus pattern was $H_2 H_1 M_1$; to present M food the pattern was $H_1 M_1 M_2$. As all
1206 channels flowed at the same rate, each occupied 1/3 of the cross-sectional flow at the worm's position with
1207 the result that small fluctuations in the position of fluidic interfaces were kept far from the worm's nose.

1208

1209 A Hamamatsu CCD camera (model C11254) controlled by HCImage was used to capture stacks of TIFF
1210 images at 10 frames/sec. Images were analyzed by manually drawing a region of interest (ROI) comprising
1211 a tightly cropped segment of the neurite connecting the cilium and soma. Mean background fluorescence
1212 was estimated from a 2-pixel thick margin situated 2 pixels outside the ROI in each frame. Absolute neu-
1213 ronral fluorescence was quantified as the mean of the 200 brightest pixels in the ROI, minus mean back-
1214 ground. Finally, fluorescence values were expressed as fractional change relative to pre-stimulus baseline
1215 absolute fluorescence. Traces shown were not bleach-corrected.

1216

1217 *Microfabrication.* Devices were fabricated using standard soft lithography (Xia and Whitesides, 1998; Xia
1218 et al., 2008). Silicon-wafer masters were created by exposing a layer of SU-8 2025 resist (Microchem,
1219 Newton, MA) through a transparency mask and developing the master in a bath of glycol monomethyl ether
1220 acetate (PGMEA). CAD files for the Y-chip and the imaging chip are provided in Supplemental Table 4.
1221 Masters were treated with tridecafluoro-1,1,2,2-tetrahydrooctyl trichlorosilane (Gelest, Morrisville, Pennsyl-
1222 vania) vapor to facilitate release. Devices were formed by casting polydimethylsiloxane pre-polymer (PDMS
1223 Sylgard 184, Dow Corning, Corning, NY) against masters. After curing and mold release, holes for external
1224 connections (fluidic inlets and outlets, worm injection, and electrodes) were formed using a 1.5 diameter
1225 punch. Devices were exposed to an air plasma then bonded to glass slides (Y-chip) or coverslips (calcium
1226 imaging chip).

1227

1228 *Statistics.* The following statistical tests were employed according to experimental design: *t*-test, two-factor
1229 analysis of variance, 2-factor analysis of variance with repeated measures on one factor. Statistical details
1230 (comparison, statistical test, degrees of freedom, *p* value) are compiled in Supplemental Table 1, and re-
1231 ferred to in the text by the notation Supplemental Table 1^{*n*}, where *n* is the row number.

1232

1233 **ACKNOWLEDGEMENTS**

1234

1235 This research was supported by MH051383 and GM129576 from the National Institutes of Health (SRL).
1236 We thank Mei Zhen for the GCaMP-6s::wCherry probe used in imaging experiments, Jonathan Millet for
1237 assistance, and Anastasia Levichev for comments on the manuscript.

1238

1239

1240 **COMPETING INTERESTS**

1241

1242 S.R.L. is co-founder and Chief Technology Officer of InVivo Biosystems, Inc., which manufactures instru-
1243 mentation for recording electropharyngeograms. The other authors have no competing interests.

1244

REFERENCES

- 1245
1246
1247 Addressi, E. *et al.* (2008) 'Preference Transitivity and Symbolic Representation in Capuchin Monkeys (*Cebus apella*)', *PLoS ONE*, 3(6), pp. 4–11. doi: 10.1371/journal.pone.0002414.
1248
1249 Afriat, S. N. (1967) 'The Construction of Utility Functions from Expenditure Data', *International Economic Review*. JSTOR, 8(1), pp. 67–77. doi: 10.2307/2525382.
1250
1251 Andreoni, J. and Miller, J. (2002) 'Giving According To Garp', *Econometrica*, 70(2), pp. 737–753.
1252 Available at: <http://www.jstor.org/stable/2692289>.
1253 Arbuthnott, D. *et al.* (2017) 'Mate choice in fruit flies is rational and adaptive', *Nature Comm*, (May 2016).
1254 doi: 10.1038/ncomms13953.
1255 Ardiel, E. L. and Rankin, C. H. (2010) 'An elegant mind: Learning and memory in *Caenorhabditis elegans*', *Learning and Memory*, pp. 191–201. doi: 10.1101/lm.960510.
1256
1257 Avery, L. and Horvitz, H. R. (1990) 'Effects of starvation and neuroactive drugs on', *Journal of Experimental Zoology*. J Exp Zool, 253(3), pp. 263–270. doi: 10.1002/jez.1402530305.
1258
1259 Avery, L. and Shtonda, B. B. (2003) 'Food transport in the *C. elegans* pharynx', *Journal of Experimental Biology*. doi: 10.1242/jeb.00433.
1260
1261 Barrios, A., Nurrish, S. and Emmons, S. W. (2008) 'Sensory Regulation of *C. elegans* Male Mate-Searching Behavior', *Current Biology*. Elsevier Ltd, 18(23), pp. 1865–1871. doi:
1262 10.1016/j.cub.2008.10.050.
1263
1264 Bendesky, A. *et al.* (2011) 'Catecholamine receptor polymorphisms affect decision-making in *C. elegans*', *Nature*. Nature Publishing Group. doi: 10.1038/nature09821.
1265
1266 Brenner, S. (1974) 'The genetics of *Caenorhabditis elegans*', *Genetics*, 77, pp. 71–94.
1267
1268 Brittin, C. A. *et al.* (2021) 'A multi-scale brain map derived from whole-brain volumetric reconstructions', *Nature*. Nature Research, 591(7848), pp. 105–110. doi: 10.1038/s41586-021-03284-x.
1269
1270 Burghart, D. R., Glimcher, P. W. and Lazzaro, S. . (2013) 'An expected utility maximizer walks into a bar...', *Journal of Risk and Uncertainty*, 46, pp. 215–246.
1271
1272 Busch, K. E. and Olofsson, B. (2012) 'Should I stay or should I go?', *Worm*, 1(3), pp. 1–5.
1273
1274 Calvo, A. C. *et al.* (2011) 'Divergence in enzyme regulation between *Caenorhabditis elegans* and human tyrosine hydroxylase, the key enzyme in the synthesis of dopamine', *Biochemical Journal*, 141, pp. 133–141. doi: 10.1042/BJ20101561.
1275
1276 Camille, N. *et al.* (2011) 'Ventromedial frontal lobe damage disrupts value maximization in humans', *Journal of Neuroscience*. doi: 10.1523/JNEUROSCI.6527-10.2011.
1277
1278 Cermak, N. *et al.* (2020) 'Whole-organism behavioral profiling reveals a role for dopamine in statedependent motor program coupling in *C. Elegans*', *eLife*, 9, pp. 1–34. doi: 10.7554/eLife.57093.
1279
1280 Chalasani, S. H. *et al.* (2007) 'Dissecting a circuit for olfactory behaviour in *Caenorhabditis elegans*', *Nature*, 450(November), pp. 63–70. doi: 10.1038/nature06292.
1281
1282 Chalfie, M. *et al.* (1985) 'The neural circuit for touch sensitivity in *Caenorhabditis elegans*', *Journal of Neuroscience*, 5(4), pp. 956–964. doi: 10.1523/jneurosci.05-04-00956.1985.
1283
1284 Choi, J. I. *et al.* (2016) 'A natural odor attraction between lactic acid bacteria and the nematode *Caenorhabditis elegans*', *ISME Journal*. Nature Publishing Group, 10(3), pp. 558–567. doi:
1285 10.1038/ismej.2015.134.
1286
1287 Chung, H.-K., Tymula, A. and Glimcher, P. (2017) 'The Reduction of Ventrolateral Prefrontal Cortex Gray Matter Volume Correlates with Loss of Economic Rationality in Aging'. doi: 10.1523/JNEUROSCI.1171-17.2017.
1288
1289 Cohen, D. *et al.* (2019) 'Bounded rationality in *C. elegans* is explained by circuit-specific normalization in chemosensory pathways', *Nature Communications*. Springer US, 10(1), pp. 1–12. doi: 10.1038/s41467-019-11715-7.
1290
1291
1292 Colbert, H. A. and Bargmann, C. I. (1995) 'Odorant-specific adaptation pathways generate olfactory plasticity in *C. elegans*', *Neuron*. doi: 10.1016/0896-6273(95)90224-4.
1293
1294 Cook, S. J. *et al.* (2019) 'Whole-animal connectomes of both *Caenorhabditis elegans* sexes', *Nature*. Springer US, 571(7763), pp. 63–71. doi: 10.1038/s41586-019-1352-7.
1295
1296 Culotti, J. and Russell, R. (1978) 'Osmotic avoidance defective mutants of the nematode *C. elegans*', *Genetics*, 90, pp. 243–256.
1297
1298 Dechaume-Moncharmont, F.-X. *et al.* (2013) 'Female mate choice in convict cichlids is transitive and consistent with a self-referent directional preference', *Frontiers in Zoology*, 10, pp. 1–10. Available at:
1299 <http://www.frontiersinzoology.com/content/10/1/69>.
1300

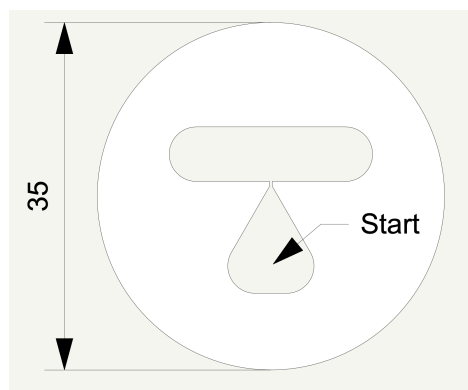
- 1301 Fang-yen, C., Avery, L. and Samuel, A. D. T. (2009) 'Two size-selective mechanisms specifically trap
1302 bacteria-sized food particles in *Caenorhabditis elegans*', *Proceedings of the National Academy of
1303 Sciences of the United States of America*, 106(47), pp. 1–4.
- 1304 Faumont, S., Lindsay, T. H. and Lockery, S. R. (2012) 'Neuronal microcircuits for decision making in *C.
1305 elegans*', *Current Opinion in Neurobiology*, pp. 580–591. doi: 10.1016/j.conb.2012.05.005.
- 1306 Faumont, S. and Lockery, S. R. (2006) 'The awake behaving worm: Simultaneous imaging of neuronal
1307 activity and behavior in intact animals at millimeter scale', *Journal of Neurophysiology*, 95(3). doi:
1308 10.1152/jn.01050.2005.
- 1309 Fréchette, G. R. (2016) 'Experimental economics across subject populations', in Kagel, J. H. and Roth, A.
1310 E. (eds) *The Handbook of Experimental Economics*. Princeton: Princeton University Press, pp. 000–000.
- 1311 Frezal, L. and Felix, M.-A. (2015) '*C. elegans* outside the Petri dish', *eLife*, pp. 1–14. doi:
1312 10.7554/eLife.05849.
- 1313 Ghosh, D. D. *et al.* (2016) 'Neural Architecture of Hunger-Dependent Multisensory Decision Making in *C.
1314 elegans*', *Neuron*. Elsevier Inc., 92(5), pp. 1049–1062. doi: 10.1016/j.neuron.2016.10.030.
- 1315 Gordus A, Pokala N, Levy S, Flavell SW, B. C. (2015) 'Feedback from network states generates variability
1316 in a probabilistic olfactory circuit', *Cell*, 161, pp. 215–227. d.
- 1317 Ha, H. *et al.* (2010) 'Article Functional Organization of a Neural Network for Aversive Olfactory Learning in
1318 *Caenorhabditis elegans*', *Neuron*, 68, pp. 1173–1186. doi: 10.1016/j.neuron.2010.11.025.
- 1319 Hammarlund, M. *et al.* (2018) 'The CeNGEN Project: The Complete Gene Expression Map of an Entire
1320 Nervous System', *Neuron*. Cell Press, pp. 430–433. doi: 10.1016/j.neuron.2018.07.042.
- 1321 Harbaugh, W. T., Krause, K. and Berry, T. R. (2001) 'GARP for Kids', *The American Economic Review*,
1322 91(5), pp. 1539–1545.
- 1323 Hendricks, M. *et al.* (2012) 'Compartmentalized calcium dynamics in a *C. elegans* interneuron encode
1324 head movement', *Nature*. Nature Publishing Group, 487, pp. 99–103. doi: 10.1038/nature11081.
- 1325 Heufer, J. (2009) *Essays on revealed preference: contributions to the theory of consumer's behavior*.
1326 Available at: <https://core.ac.uk/download/pdf/46909503.pdf>.
- 1327 Hobert, O. (2021) *Neurotransmitter map*. Available at: <https://www.hobertlab.org/neurotransmitter-map/>.
- 1328 Hoenderop, J. G. J. *et al.* (1999) 'The epithelial calcium channel, ECaC, is activated by hyperpolarization
1329 and regulated by cytosolic calcium', *Biochemical and Biophysical Research Communications*, 261(2), pp.
1330 488–492. doi: 10.1006/bbrc.1999.1059.
- 1331 Houthakker, H. S. (1950) 'Revealed preference theory a tthe utility function', *Economica*, 17, pp. 159–
1332 174.
- 1333 Huguenard, J. R. and McCormick, D. A. (2007) 'Thalamic synchrony and dynamic regulation of global
1334 forebrain oscillations', *Trends in Neurosciences*, 30(7), pp. 350–356. doi: 10.1016/j.tins.2007.05.007.
- 1335 Hukema, R. K., Rademakers, S. and Jansen, G. (2008) 'Gustatory plasticity in *C. elegans* involves
1336 integration of negative cues and NaCl taste mediated by serotonin, dopamine, and glutamate', *Learning
1337 and Memory*, 15(11), pp. 829–836. doi: 10.1101/lm.994408.
- 1338 Iino, Y. and Yoshida, K. (2009) 'Parallel Use of Two Behavioral Mechanisms for Chemotaxis in
1339 *Caenorhabditis elegans*', *Journal of Neuroscience*, 29(17), pp. 5370–5380. doi:
1340 10.1523/JNEUROSCI.3633-08.2009.
- 1341 Iwanir, S. *et al.* (2019) 'Irrational behavior in *C. elegans* arises from asymmetric modulatory effects within
1342 single sensory neurons', *Nature Communications*. Springer US, 10(1). doi: 10.1038/s41467-019-11163-3.
- 1343 Jarrell, T. A. *et al.* (2012) 'The connectome of a decision-making neural network.', *Science (New York,
1344 N.Y.)*. American Association for the Advancement of Science, 337(6093), pp. 437–44. doi:
1345 10.1126/science.1221762.
- 1346 Jevons, W. . (1871) *The Theory of Political Economy*. London.: Macmillan and Co.
- 1347 Kacelnik, A. (2006) 'Minimal rationality', in Hurley, S. L. and Nudds, M. (eds) *Rational Animals?* Oxford:
1348 Oxford University Press, pp. 87–106.
- 1349 Kagel, J. *et al.* (1975) 'Experimental studies of consumer demand behavior using laboratory animals',
1350 *Economic Inquiry*, 13(1), pp. 22–38.
- 1351 Kagel, J. H. *et al.* (1981) 'Demand curves for animal consumers', *Quarterly Journal of Economics*, 96(1),
1352 pp. 1–15.
- 1353 Kagel, J. H., Battalio, R. C. and Green, L. (1995) *Economic Choice Theory*. Cambridge: Cambridge
1354 University Press.
- 1355 Kalenscher, T., Wingerden, M. Van and Hayden, B. (2011) 'Why we should use animals to study
1356 economic decision making – a perspective', *Frontiers in Neuroscience*, 5(June), pp. 1–11. doi:

- 1357 10.3389/fnins.2011.00082.
- 1358 Kato, S. *et al.* (2013) 'Article Temporal Responses of C. elegans Chemosensory Neurons Are Preserved
- 1359 in Behavioral Dynamics', *Neuron*. Elsevier Inc., 81(3), pp. 616–628. doi: 10.1016/j.neuron.2013.11.020.
- 1360 Kato, S. *et al.* (2015) 'Global Brain Dynamics Embed the Motor Command Sequence of Caenorhabditis
- 1361 elegans', *Cell*, 163(3). doi: 10.1016/j.cell.2015.09.034.
- 1362 Keane, J. and Avery, L. (2003) 'Mechanosensory Inputs Influence Caenorhabditis elegans Pharyngeal
- 1363 Activity via Ivermectin Sensitivity Genes', *Genetics*, 164(May), pp. 153–162.
- 1364 Kocabas, A. *et al.* (2012) 'elegans to evoke chemotactic behaviour', *Nature*. Nature Publishing Group,
- 1365 490(7419), pp. 273–277. doi: 10.1038/nature11431.
- 1366 Koch, A. L. (1970) 'Turbidity measure of bacterial cultures in some available commercial instruments',
- 1367 *Analytical Biochemistry*, 1, pp. 252–259.
- 1368 Koga, M. and Ohshima, Y. (2004) 'The C. elegans ceh-36 Gene Encodes a Putative Homemodomain
- 1369 Transcription Factor Involved in Chemosensory Functions of ASE and AWC Neurons', *Journal of*
- 1370 *Molecular Biology*, 336, pp. 579–587. doi: 10.1016/j.jmb.2003.12.037.
- 1371 Kopp-Scheinflug, C., Sinclair, J. L. and Linden, J. F. (2018) 'When Sound Stops: Offset Responses in
- 1372 the Auditory System', *Trends in Neurosciences*, 41(10), pp. 712–728. doi: 10.1016/j.tins.2018.08.009.
- 1373 Lanjuin, A. *et al.* (2003) 'Otx / otd Homeobox Genes Specify Distinct Sensory Neuron Identities in C.
- 1374 elegans', *Developmental Cell*, 5, pp. 621–633.
- 1375 Latty, T. and Beekman, M. (2011) 'Irrational decision-making in an amoeboid organism: transitivity and
- 1376 context-dependent preferences', *Proceeding of the Royal Society B*, 278(August 2010), pp. 307–312. doi:
- 1377 10.1098/rspb.2010.1045.
- 1378 Lazzaro, S. C. *et al.* (2016) 'The impact of menstrual cycle phase on economic choice and rationality',
- 1379 *PLoS ONE*. Public Library of Science, 11(1). doi: 10.1371/journal.pone.0144080.
- 1380 Lee, J., Jee, C. and McIntire, S. L. (2009) 'Ethanol preference in C. elegans', *Genes, Brain and Behavior*,
- 1381 8(6), pp. 578–585. doi: 10.1111/j.1601-183X.2009.00513.x.
- 1382 Lee, K. S. *et al.* (2017) 'Serotonin-dependent kinetics of feeding bursts underlie a graded response to
- 1383 food availability in C. elegans', *Nature Communications*. Nature Publishing Group, 8, pp. 1–11. doi:
- 1384 10.1038/ncomms14221.
- 1385 Lints, R. and Emmons, S. W. (1999) 'Patterning of dopaminergic neurotransmitter identity among
- 1386 Caenorhabditis elegans ray sensory neurons by a TGF β family signaling pathway and a Hox gene',
- 1387 *Development*, 5831, pp. 5819–5831.
- 1388 Lockery, S. R. *et al.* (2012) 'A microfluidic device for whole-animal drug screening using
- 1389 electrophysiological measures in the nematode C. elegans', *Lab on a Chip*, 12(12). doi:
- 1390 10.1039/c2lc00001f.
- 1391 Mazur, J. E. and Coe, D. (1987) 'Test of transitivity in choices between fixed and variable reinforcer
- 1392 delays', *Journal of the Experimental Analysis of Behavior*, 47, pp. 287–297.
- 1393 McCormick, K. E. *et al.* (2011) 'Microfluidic devices for analysis of spatial orientation behaviors in semi-
- 1394 restrained Caenorhabditis elegans', *PLoS ONE*, 6(10). doi: 10.1371/journal.pone.0025710.
- 1395 Milward, K. *et al.* (2011) 'Neuronal and molecular substrates for optimal foraging in Caenorhabditis
- 1396 elegans'. doi: 10.1073/pnas.1106134109/-
- 1397 /DCSupplemental.www.pnas.org/cgi/doi/10.1073/pnas.1106134109.
- 1398 Musselman, H. N. *et al.* (2012) 'Chemosensory cue conditioning with stimulants in a Caenorhabditis
- 1399 elegans animal model of addiction', *Behavioral Neuroscience*, 126(3), pp. 445–456. doi:
- 1400 10.1037/a0028303.
- 1401 Nehrke, K. *et al.* (2000) 'Model Organisms: New Insights Into Ion Channel and Transporter Function.
- 1402 Caenorhabditis elegans CIC-type chloride channels: novel variants and functional expression', *American*
- 1403 *Journal of Cell Physiology*, 279, pp. C2052–C2066. doi: 10.1007/978-3-030-53953-5_10.
- 1404 Nguyen, J. P. *et al.* (2016) 'Whole-brain calcium imaging with cellular resolution in freely behaving
- 1405 Caenorhabditis elegans', *Proceedings of the National Academy of Sciences of the United States of*
- 1406 *America*, 113(8), pp. E1074–E1081. doi: 10.1073/pnas.1507110112.
- 1407 Nickell, W. T. *et al.* (2002) 'Single ionic channels of two Caenorhabditis elegans chemosensory neurons
- 1408 in native membrane', *Journal of Membrane Biology*, 189(1), pp. 55–66. doi: 10.1007/s00232-002-1004-x.
- 1409 Nilius, B. *et al.* (2000) 'Whole-cell and single channel monovalent cation currents through the novel rabbit
- 1410 epithelial Ca²⁺ channel ECaC', *Journal of Physiology*, 527(2), pp. 239–248. doi: 10.1111/j.1469-
- 1411 7793.2000.00239.x.
- 1412 Padoa-schioppa, C. and Assad, J. A. (2006) 'Neurons in the orbitofrontal cortex encode economic value',

- 1413 *Nature*, 441(May), pp. 223–226. doi: 10.1038/nature04676.
- 1414 Pastor-Bernier, A., Stasiak, A. and Schultz, W. (2019) 'Orbitofrontal signals for two-component choice
1415 options comply with indifference curves of Revealed Preference Theory', *Nature Communications*, 10(1).
1416 doi: 10.1038/s41467-019-12792-4.
- 1417 Pearson, J. M., Watson, K. K. and Platt, M. L. (2014) 'Decision Making : The Neuroethological Turn',
1418 *Neuron*, 82(June), pp. 950–965.
- 1419 Press, W. H. *et al.* (2007) *Numerical Recipes*. 3rd edn. Cambridge University Press.
- 1420 Raible, F. and Arendt, D. (2004) 'Metazoan Evolution: Some Animals Are More Equal than Others',
1421 *Current Biology*, 14(3), pp. R106–R108. doi: 10.1016/j.cub.2004.01.015.
- 1422 Raizen, D. M. and Avery, L. (1994) 'Electrical Activity and Behavior in the Pharynx of *Caenorhabditis*
1423 *elegans*', *Neuron*, 12, pp. 483–495.
- 1424 Roberts, A., Li, W. C. and Soffe, S. R. (2008) 'Roles for inhibition: Studies on networks controlling
1425 swimming in young frog tadpoles', *Journal of Comparative Physiology A: Neuroethology, Sensory,*
1426 *Neural, and Behavioral Physiology*, 194(2), pp. 185–193. doi: 10.1007/s00359-007-0273-3.
- 1427 Rose, H. (1958) 'Consistency of Preference : The Two-Commodity Case', *The Review of Economic*
1428 *Studies*, 25(2), pp. 124–125.
- 1429 Saeki, S., Yamamoto, M. and Iino, Y. (2001) 'Plasticity of chemotaxis revealed by paired presentation of a
1430 chemoattractant and starvation in the nematode *Caenorhabditis elegans*', *Journal of Experimental*
1431 *Biology*, 204(10), pp. 1757–1764.
- 1432 Samuel, B. S. *et al.* (2016) '*Caenorhabditis elegans* responses to bacteria from its natural habitats',
1433 *Proceedings of the National Academy of Sciences of the United States of America*, pp. E3941–E3949.
1434 doi: 10.1073/pnas.1607183113.
- 1435 Samuelson, P. A. (1938) 'A note on the pure theory of consumer's behaviour', *Economica*, 51(17), pp.
1436 61–71.
- 1437 Sawin, E. R., Ranganathan, R. and Horvitz, H. R. (2000) 'C. *elegans* locomotory rate is modulated by the
1438 environment through a dopaminergic pathway and by experience through a serotonergic pathway',
1439 *Neuron*. doi: 10.1016/S0896-6273(00)81199-X.
- 1440 Scholz, M. *et al.* (2016) 'A scalable method for automatically measuring pharyngeal pumping in C .
1441 *elegans*', *Journal of Neuroscience Methods*. Elsevier B.V., 274, pp. 172–178. doi:
1442 10.1016/j.jneumeth.2016.07.016.
- 1443 Schuck-Paim, C. and Kacelnik, A. (2002) 'Rationality in risk-sensitive foraging choices by starlings',
1444 *Animal Behaviour*, 64, pp. 869–879. doi: 10.1006/anbe.2002.2003.
- 1445 Senior, N. (1836) *An Outline of the Science of Political Economy*. London: Encyclopaedia Metropolitana.
- 1446 Shafir, S. (1994) 'Intransitivity of preferences in honey bees: support of "comparative" evaluation of
1447 foraging options', *Animal Behaviour*, 48, pp. 55–67.
- 1448 Shinkai, Y., Yamamoto, Y., Fujiwara, M., Tabata, T., Murayama, T., Hirotsu, T., Ikeda, Daisuke D., *et al.*
1449 (2011) 'Behavioral choice between conflicting alternatives is regulated by a receptor guanylyl cyclase,
1450 GCY-28, and a receptor tyrosine kinase, SCD-2, in AIA interneurons of *Caenorhabditis elegans*', *Journal*
1451 *of Neuroscience*, 31(8), pp. 3007–3015. doi: 10.1523/JNEUROSCI.4691-10.2011.
- 1452 Shinkai, Y., Yamamoto, Y., Fujiwara, M., Tabata, T., Murayama, T., Hirotsu, T., Ikeda, Daisuke D, *et al.*
1453 (2011) 'Cellular/Molecular Behavioral Choice between Conflicting Alternatives Is Regulated by a Receptor
1454 Guanylyl Cyclase, GCY-28, and a Receptor Tyrosine Kinase, SCD-2, in AIA Interneurons of
1455 *Caenorhabditis elegans*'. doi: 10.1523/JNEUROSCI.4691-10.2011.
- 1456 Shtonda, B. B. and Avery, L. (2006) 'Dietary choice behavior in *Caenorhabditis elegans*', *Journal of*
1457 *Experimental Biology*. doi: 10.1242/jeb.01955.
- 1458 Simon, H. A. (1957) *Models of Man*. New York: Wiley.
- 1459 Song, B.-M. *et al.* (2013) 'Recognition of familiar food activates feeding via an endocrine serotonin signal
1460 in *Caenorhabditis elegans*', *eLife*, 2013(2). doi: 10.7554/eLife.00329.
- 1461 Stevenson, K. *et al.* (2016) 'General calibration of microbial growth in microplate readers', *Scientific*
1462 *Reports*, 6, 6, p. 38828.
- 1463 Sumpter, C. E., Temple, W. and Foster, T. . (1999) 'The transitivity of choices between different response
1464 requirements', *Journal of the Experimental Analysis of Behavior*, 72(2), pp. 235–249.
- 1465 Tan, M. *et al.* (1999) '*Pseudomonas aeruginosa* killing of *Caenorhabditis elegans* used to identify P.
1466 *aeruginosa* virulence factors', 96, pp. 2408–2413. Available at: www.pnas.org.
- 1467 Tanimoto, Y. *et al.* (2016) 'In actio optophysiological analyses reveal functional diversification of
1468 dopaminergic neurons in the nematode C. *elegans*', *Scientific Reports*. doi: 10.1038/srep26297.

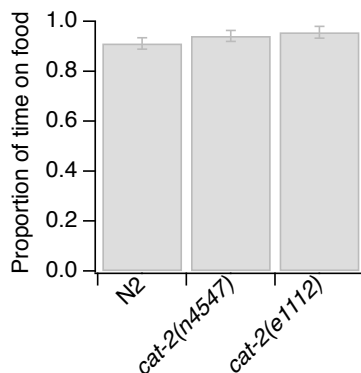
- 1469 Torayama, I., Ishihara, T. and Katsura, I. (2007) 'Caenorhabditis elegans Integrates the Signals of
1470 Butanone and Food to Enhance Chemotaxis to Butanone', *27*(4), pp. 741–750. doi:
1471 10.1523/JNEUROSCI.4312-06.2007.
- 1472 Varian, H. R. (1982) 'The Nonparametric Approach to Demand Analysis', *Econometrica*, *50*(4), pp. 945–
1473 973.
- 1474 Varian, H. R. (1992) *Microeconomic Analysis*. 3rd edn. W. W. Norton & Company.
- 1475 Varian, H. R. (1995) 'Efficiency in production and consumption'.
- 1476 Venkatachalam, V. *et al.* (2016) 'Pan-neuronal imaging in roaming *Caenorhabditis elegans*', *Proceedings*
1477 *of the National Academy of Sciences of the United States of America*, *113*(8), pp. E1082–E1088. doi:
1478 10.1073/pnas.1507109113.
- 1479 Voglis, G. and Tavernarakis, N. (2008) 'A synaptic DEG/ENaC ion channel mediates learning in *C.*
1480 *elegans* by facilitating dopamine signalling', *EMBO Journal*, *27*(24), pp. 3288–3299. doi:
1481 10.1038/emboj.2008.252.
- 1482 W K Bickel, L Green, R. E. V. (1995) 'Behavioral economics', *J Exp Anal Behav*, *64*(3)(3), pp. 257–62.
- 1483 Weeks, J. C. *et al.* (2018) 'Anthelmintic drug actions in resistant and susceptible *C. elegans* revealed by
1484 electrophysiological recordings in a multichannel microfluidic device', *International Journal for*
1485 *Parasitology: Drugs and Drug Resistance*, *8*(3). doi: 10.1016/j.ijpddr.2018.10.003.
- 1486 Wes, P. D. and Bargmann, C. I. (2001) '*C. elegans* odour discrimination requires asymmetric diversity in
1487 olfactory neurons', *Nature*, *410*(April), pp. 10–13.
- 1488 White JG, Southgate E, Thomson JN, B. S. (1986) 'The structure of the nervous system of the nematode
1489 *Caenorhabditis elegans*', *Philosophical Transactions of the Royal Society of London. B, Biological*
1490 *Sciences*. The Royal Society, *314*(1165), pp. 1–340. doi: 10.1098/rstb.1986.0056.
- 1491 Worthy, S. E., Haynes, L., *et al.* (2018) 'Identification of attractive odorants released by preferred bacterial
1492 food found in the natural habitats of *C. elegans*', *PLoS ONE*, pp. 1–14. Available at:
1493 <https://doi.org/10.1371/journal.pone.0201158>.
- 1494 Worthy, S. E., Rojas, G. L., *et al.* (2018) 'Identification of Odor Blend Used by *Caenorhabditis elegans* for
1495 Pathogen Recognition', *Chemical Senses*, *43*(January), pp. 169–180. doi: 10.1093/chemse/bjy001.
- 1496 Xia, Y. *et al.* (2008) 'Complex Optical Surfaces Formed by Replica Molding Against Elastomeric Masters
1497 Published by : American Association for the Advancement of Science Stable URL :
1498 <http://www.jstor.org/stable/2889746>', *273*(5273), pp. 347–349.
- 1499 Xia, Y. and Whitesides, G. M. (1998) 'Soft lithography', *Angewandte Chemie - International Edition*, *37*(5),
1500 pp. 550–575. doi: 10.1002/(sici)1521-3773(19980316)37:5<550::aid-anie550>3.3.co;2-7.
- 1501 Yapici, N., Zimmer, M. and Domingos, A. I. (2014) 'Cellular and molecular basis of decision-making',
1502 *EMBO reports*. EMBO, *15*(10), pp. 1023–1035. doi: 10.15252/embr.201438993.
- 1503 Zaslaver, A. *et al.* (2015) 'Hierarchical sparse coding in the sensory system of *Caenorhabditis elegans*',
1504 *Proceedings of the National Academy of Sciences of the United States of America*, *112*(4), pp. 1185–
1505 1189. doi: 10.1073/pnas.1423656112.
- 1506 Zhang, Y., Lu, H. and Bargmann, C. I. (2005) 'Pathogenic bacteria induce aversive olfactory learning in
1507 *Caenorhabditis elegans*', *438*(November), pp. 179–184. doi: 10.1038/nature04216.
- 1508

1509 **SUPPLEMENTARY INFORMATION**
1510



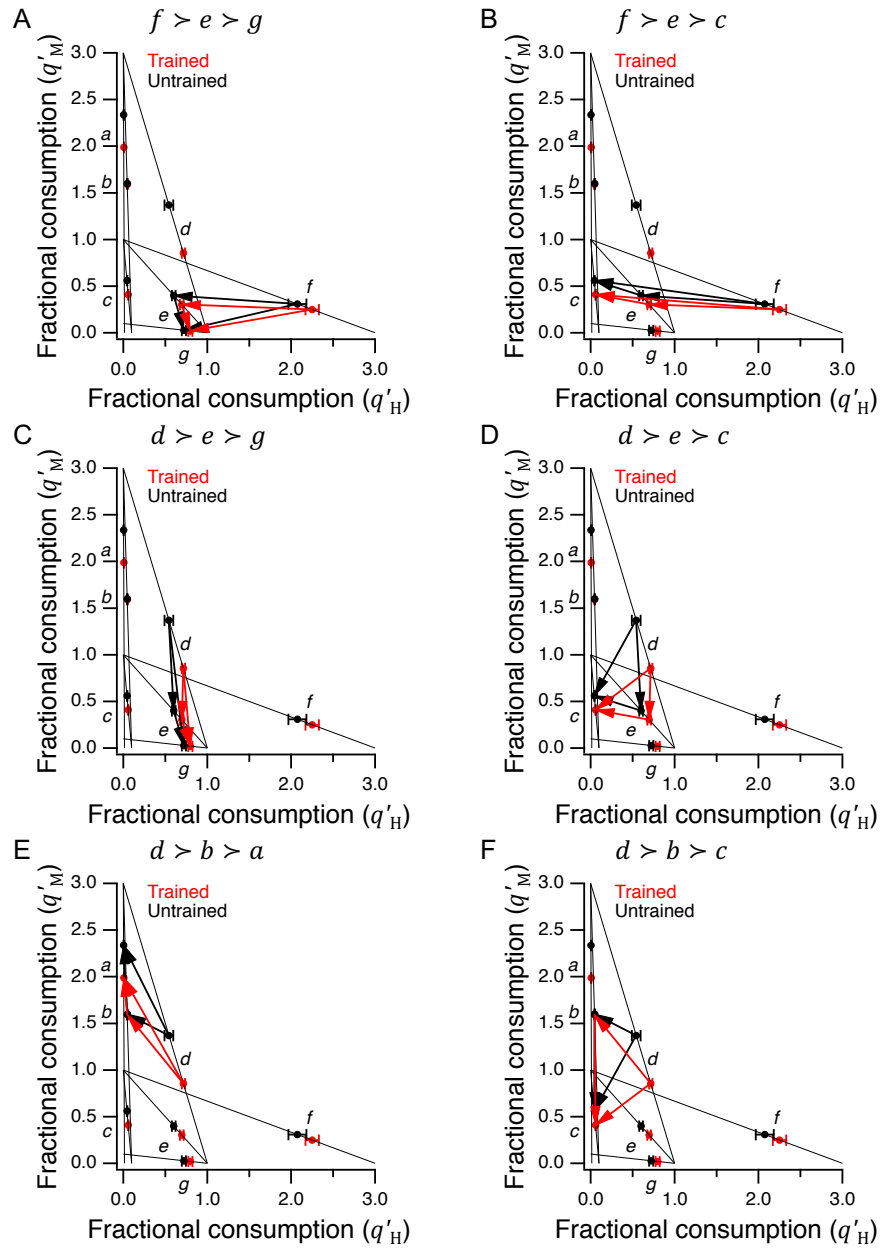
1511 **Supplemental Figure 1: T-maze**

1512 The teardrop shaped feature acts as worm diode. Worms leave the teardrop more easily than they re-
1513 enter it, thus helping to ensure they do not congest at the starting point. The mask's ability to confine
1514 worms in the test area is improved by floating the maze on the surface of the agarose medium while it is
1515 still liquid (M. Brooks, pers. comm.). Dimensions are in mm.
1516
1517
1518
1519



1520 **Supplemental Figure 2: Loss of dopamine signaling does not reduce proportion of time on food**

1521 Mutations in the gene *cat-2* do not significantly alter the ability of worms to find and remain in food
1522 patches. Statistics (*t*-tests): N2 vs. *cat-2*(n4547), $t(38) = -0.95$, $P = 0.35$; N2 vs *cat-2*(e1112), $t(40) = -1.38$,
1523 $P = 0.18$.
1524
1525
1526
1527



1528

1529

Supplemental Figure 3. Indirectly revealed preferences inherent in the choices shown in Fig. 5C

1530

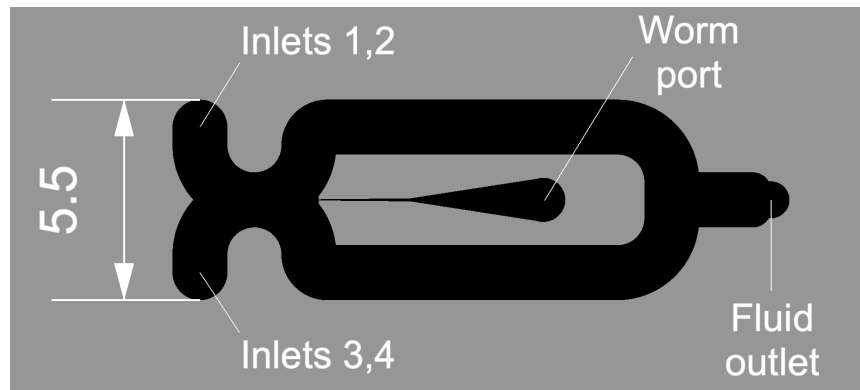
1531

1532

1533

1534

A-F. Italic lower case letters refer to the preferred option in each choice set, consistent with the labels in Fig. 5B,C. Arrows show pairwise preferences implied by the data set, such that $i \rightarrow j$ means $i > j$. There are no transitivity violations in that, for each triplet $i > j > k$, the arrow between the first and third option points in the direction $i \rightarrow k$, rather than $k \rightarrow i$.



1535
1536
1537
1538
1539
1540

Supplemental Figure 4: Imaging chip

Fluidic features are shown in black. Dimensions are in mm.

Row	Figure	Test	Comparison	Statistic	DF1	DF2	P
1	2B*	Two-factor ANOVA, repeated measures, posthoc t-tests	N2, Trained vs. Untrained, post-hoc <i>t</i> -tests	<i>t</i> 2.50	7	–	2.96E-02
2	2B	<i>t</i> -test	N2, Untrained, 60 min mean <i>I</i> > 0	<i>t</i> 10.21	7	–	1.86E-05
3	2B	<i>t</i> -test	<i>ceh-36</i> , Untrained, 60 min mean <i>I</i> > 0	<i>t</i> 3.58	7	–	9.00E-03
4	2B	Two-factor ANOVA, repeated measures, main effect	Trained <i>ceh-36</i> vs. N2 Untrained	<i>F</i> 0.11	1	14	2.50E-01
5	2B	Two-factor ANOVA, repeated measures, main effect	Untrained <i>ceh-36</i> vs. N2 Untrained	<i>F</i> 2.50	1	14	1.74E-01
6	2B	Two-factor ANOVA, repeated measures, main effect	<i>ceh-36</i> , Trained vs. Untrained	<i>F</i> 0.66	1	14	5.70E-01
7	2C	Two-factor ANOVA, repeated measures, main effect	Azide-, Trained vs. Untrained	<i>F</i> 11.28	1	21	2.98E-03
8	2C	<i>t</i> -test	Azide+, Trained, 60 min mean <i>I</i> > 0	<i>t</i> 6.35	10	–	8.36E-05
9	2C	<i>t</i> -test	Azide+, Untrained, 60 min mean <i>I</i> > 0	<i>t</i> 3.09	10	–	1.15E-02
10	2C	Two-factor ANOVA, repeated measures, main effect	Azide+, Trained vs. Untrained	<i>F</i> 10.32	1	20	4.37E-03
11	2C	Two-factor ANOVA, repeated measures, main effect	Trained, Azide+ vs. Azide–	<i>F</i> 11.17	1	19	3.43E-03
12	2C	Two-factor ANOVA, repeated measures, main effect	Untrained, Azide+ vs. Azide–	<i>F</i> 38.28	1	22	3.16E-06
13	2D	Two-factor ANOVA, repeated measures, main effect	Untrained, N2 vs. <i>cat-2</i>	<i>F</i> 23.25	1	21	9.14E-05
14	2D	Two-factor ANOVA, repeated measures, main effect	Trained, N2 vs. <i>cat-2</i>	<i>F</i> 52.50	1	18	9.74E-07
15	2D	Two-factor ANOVA, repeated measures, main effect	<i>cat-2</i> , Trained vs. Untrained	<i>F</i> 0.90	1	18	6.43E-01
16	4A	Two-factor ANOVA, main effect	Familiar vs. unfamiliar	<i>F</i> 10.46	1	27	2.1E-03
17	4A	<i>t</i> -test	Unfamiliar, grown in H vs. grown in M	<i>t</i> 1.77	17	–	9.4E-02
18	4B	<i>t</i> -test	Trained, <i>f</i> _H > 0.5	<i>t</i> 8.60	18	–	8.6E-08
19	4B	<i>t</i> -test	Trained, <i>f</i> _H > 0.5	<i>t</i> 4.35	27	–	1.7E-04
20	4B*	<i>t</i> -test	Trained vs. Untrained	<i>t</i> 3.06	45	–	3.75E-03
21	4E	Two-factor ANOVA, main effect	Peak Frequency vs. Optical Density	<i>F</i> 31.58	3	108	P < .001
22	4F	Two-factor ANOVA, main effect	Time to Half-max Pumping Rate vs. Optical Density	<i>F</i> 3.10	3	106	3.00E-02
23	5B	Two-factor ANOVA, main effect	Effect of price ratio	<i>F</i> 3.97	6	191	1.0E-03
24	5B	Two-factor ANOVA, main effect	Trained vs. Untrained	<i>F</i> 39.30	18	191	1.0E-03
25	5B	<i>t</i> -test	Trained, point <i>a</i> , mean <i>f</i> _H < 0.5	<i>t</i> 6.22	8	–	2.52E-04
26	5B	<i>t</i> -test	Untrained, point <i>a</i> , mean <i>f</i> _H < 0.5	<i>t</i> 8.29	11	–	4.66E-06
27	6A	Regression with replication slope test	Fig. 5B, points <i>abd</i> , Trained slope ≠ 0	<i>F</i> 118.79	1	47	1.85E-14
28	6A	Regression with replication slope test	Fig. 5B, points <i>abd</i> , Untrained slope ≠ 0	<i>F</i> 28.52	1	39	4.26E-06
29	6A	Regression with replication slope test	Fig. 5B, points <i>cef</i> , Trained slope ≠ 0	<i>F</i> 20.29	1	46	4.54E-05
30	6A	Regression with replication slope test	Fig. 5B, points <i>cef</i> , Untrained slope ≠ 0	<i>F</i> 26.56	1	49	4.55E-06
31	6A	Regression with replication slope test	Fig. 5B, points <i>deg</i> , Trained slope ≠ 0	<i>F</i> 2.34	1	51	1.32E-01
32	6A	Regression with replication slope test	Fig. 5B, points <i>deg</i> , Untrained slope ≠ 0	<i>F</i> 7.82	1	45	7.56E-03
33	7A	Regression	Frequency ratio vs. <i>f</i> _H	<i>t</i> -6.64	141	–	6.53E-10
34	7B	Regression	Dwell time ratio vs. <i>f</i> _H	<i>t</i> 39.60	202	–	6.95E-97
35	7C	Regression	Dwell time ratio vs. mean head angle	<i>t</i> 35.96	202	–	2.62E-89
36	7D	<i>t</i> -test	<i>ceh-36</i> Untrained, <i>f</i> _H > 0.5	<i>t</i> 4.20	10	–	1.84E-03
37	7D*	Two-factor ANOVA	Treatment × Strain interaction	<i>F</i> 5.03	1	62	2.85E-02
38	7D	<i>t</i> -test	<i>ceh-36</i> , Trained vs. Untrained	<i>t</i> -0.58	16	–	5.68E-01
39	8B	Two-factor ANOVA, main effect	Fig. 8B, mean integrated <i>dF/F</i> , H vs. M food	<i>F</i> 3.56	1	23	7.20E-02
40	8D	Two-factor ANOVA, main effect	Fig. 8D, mean integrated <i>dF/F</i> , H vs. M food	<i>F</i> 18.42	1	25	2.00E-04
41	8C*	<i>t</i> -test	Peak response, Untrained, H vs. M food	<i>t</i> 2.98	12	–	1.30E-02
42	8C*	<i>t</i> -test	Peak response, Trained, H vs. M food	<i>t</i> 3.18	13	–	7.30E-03
43	8B	Two-factor ANOVA, main effect	Trained vs. Untrained	<i>F</i> 0.00	1	23	9.90E-01
44	8D	Two-factor ANOVA, main effect	Trained vs. Untrained	<i>F</i> 7.52	1	25	1.10E-02
45	8D*	<i>t</i> -test	H food, Trained vs. Untrained	<i>t</i> 2.86	12	–	1.44E-02
46	8D	<i>t</i> -test	M food, Trained vs. Untrained	<i>t</i> -0.80	13	–	4.39E-01
47	9A*	<i>t</i> -test	H → M, peak response, Trained vs. Untrained	<i>t</i> 2.21	97	–	3.00E-02
48	9A	<i>t</i> -test	M → H, max response, Trained vs. Untrained	<i>t</i> 0.60	100	–	5.50E-01
49	9C	<i>t</i> -test	Trained, point <i>e</i> vs. Untrained, point <i>d</i>	<i>t</i> 2.14	25	–	4.23E-02

Supplemental Table 1. Statistics

P values associated with significant results are shown in bold font.

	Trained	Untrained
Offer value H	$w_T \cdot d_H$	$w_U \cdot d_H$
Log offer value H	$\log(w_T \cdot d_H)$	$\log(w_U \cdot d_H)$
Offer value M	d_M	d_M
Log offer value M	$\log(d_M)$	$\log(d_M)$
Offer value	$w_T \cdot d_H + d_M$	$w_U \cdot d_H + d_M$
Log offer value	$\log(w_T \cdot d_H + d_M)$	$\log(w_U \cdot d_H + d_M)$
Δ Offer value	$-w_T \cdot d_H + d_M$	$-w_U \cdot d_H + d_M$
Δ Log offer value	$-\log(w_T \cdot d_H) + \log(d_M)$	$-\log(w_U \cdot d_H) + \log(d_M)$
Chosen value	$w_T \cdot f_H \cdot d_H + (1 - f_H) \cdot d_M$	$w_U \cdot f_H \cdot d_H + (1 - f_H) \cdot d_M$
Log chosen value	$\log(w_T \cdot f_H \cdot d_H + (1 - f_H) \cdot d_M)$	$\log(w_U \cdot f_H \cdot d_H + (1 - f_H) \cdot d_M)$
Δ Chosen value	$-w_T \cdot f_H \cdot d_H + (1 - f_H) \cdot d_M$	$-w_U \cdot f_H \cdot d_H + (1 - f_H) \cdot d_M$
Δ Log chosen value	$-\log(w_T \cdot f_H \cdot d_H) + \log((1 - f_H) \cdot d_M)$	$-\log(w_U \cdot f_H \cdot d_H) + \log((1 - f_H) \cdot d_M)$
Offer utility H	$U_T(d_H, 0)$	$U_U(d_H, 0)$
Offer utility M	$U_T(0, d_M)$	$U_U(0, d_M)$
Offer utility	$U_T(d_H, d_M)$	$U_U(d_H, d_M)$
Δ Offer utility	$-U_T(d_H, 0) + U_T(0, d_M)$	$-U_U(d_H, 0) + U_U(0, d_M)$
Chosen utility	$U_T(f_H \cdot d_H, (1 - f_H) \cdot d_M)$	$U_U(f_H \cdot d_H, (1 - f_H) \cdot d_M)$
Δ Chosen utility	$-U_T(f_H \cdot d_H, 0) + U_T(0, (1 - f_H) \cdot d_M)$	$-U_U(f_H \cdot d_H, 0) + U_U(0, (1 - f_H) \cdot d_M)$

1542
1543
1544
1545
1546
1547
1548
1549

Supplemental Table 2: Linear correlation equations

These equations show how the economic variables in the left column were computed based on food type and density in trained and untrained animals. The quantities w_T and w_U are defined in equation 13 in the main text. The quantities U_T and U_U are, respectively, utility in trained and untrained animals computed according to the CES function as fitted to the data in Fig. 6C,D.

	Trained					Untrained				
	r^2	F	DF1	DF2	P	r^2	F	DF1	DF2	P
Offer value H	0.004	0.021	1	5	0.891	0.017	0.086	1	5	0.781
Log offer value H	0.255	1.710	1	5	0.248	0.134	0.774	1	5	0.419
Offer value M	0.106	0.594	1	5	0.476	0.005	0.027	1	5	0.875
Log offer value M	0.017	0.087	1	5	0.780	0.010	0.049	1	5	0.834
Offer value	0.003	0.014	1	5	0.912	0.015	0.077	1	5	0.793
Log offer value	0.174	1.053	1	5	0.352	0.046	0.240	1	5	0.645
Δ Offer value	0.006	0.029	1	5	0.872	0.017	0.089	1	5	0.778
Δ Log offer value	0.174	1.053	1	5	0.352	0.046	0.240	1	5	0.645
Chosen value	0.001	0.003	1	5	0.959	0.000	0.002	1	5	0.968
Log chosen value	0.098	0.541	1	5	0.495	0.007	0.035	1	5	0.858
Δ Chosen value	0.004	0.019	1	5	0.896	0.013	0.068	1	5	0.805
Δ Log chosen value	0.199	1.241	1	5	0.316	0.059	0.314	1	5	0.600
Offer utility H	0.162	0.965	1	5	0.371	0.098	0.541	1	5	0.495
Offer utility M	0.035	0.183	1	5	0.687	0.003	0.016	1	5	0.903
Offer utility	0.139	0.804	1	5	0.411	0.147	0.865	1	5	0.395
Δ Offer utility	0.151	0.890	1	5	0.389	0.043	0.225	1	5	0.655
Chosen utility	0.125	0.715	1	5	0.436	0.130	0.749	1	5	0.426
Δ Chosen utility	0.105	0.586	1	5	0.478	0.130	0.749	1	5	0.426

1550
1551 **Supplemental Table 3: Tests of linear correlations between AWC activation and economic variable**
1552 **it might hypothetically represent**
1553

1554 Significance of correlations was tested using the F distribution. This table shows, for each economic vari-
1555 able tested, the correlation coefficient, value of the F statistic, its two degrees of freedom, and the corre-
1556 sponding P value. No significant correlations were found. Definitions of variable are provided in Supple-
1557 mental Table 2.
1558

1559

T-maze	https://www.dropbox.com/s/xxy5ttfqtnglv56/T-maze-CAD.dwg?dl=0
Y-chip	https://www.dropbox.com/s/sw8df35mcy03ymz/Y-chip-CAD.dwg?dl=0
Imaging-chip	https://www.dropbox.com/s/1z7ne8crarzbk5f/Imaging-chip-CAD.dwg?dl=0

1560

1561 **Supplementary Table 4: CAD Files**

1562

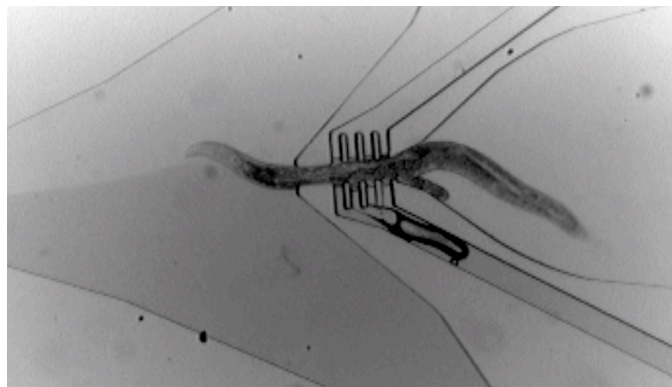
1563

1564

1565

1566

1567



1568

1569

1570 **Supplementary Video 1: Foraging behavior in the Y-chip**

1571

1572 The worms held at its midsection by a vacuum activated clamp, leaving the head (left) and tail free to
1573 move. Bubbles originating at the clamp are formed by air that has been pulled through the PDMS walls of
1574 the chip by the vacuum. The fluid streams contain M9 buffer, flowing to the left. Food dye was added to
1575 the lower stream to visualize the interface between streams. The worm prefers the dye as it contains po-
1576 tassium sorbate, which acts as a chemoattractant.

1577

1578 <https://www.dropbox.com/s/h307zd8g3nsv4cc/Y-chip-video.mov?dl=0>

1579

1580

1581

1582